Targeting TSLP: Novel Therapeutics for the Treatment of Atopic Dermatitis

by

Leah Mappalakayil

B.Sc., McGill University, 2021

A THESIS SUBMITTED IN PARTIAL FULFILLMENT OF THE REQUIREMENTS FOR

THE DEGREE OF

MASTER OF SCIENCE

in

THE FACULTY OF GRADUATE AND POSTDOCTORAL STUDIES

(Pharmaceutical Sciences)

THE UNIVERSITY OF BRITISH COLUMBIA

(Vancouver)

December 2023

The following individuals certify that they have read, and recommend to the Faculty of Graduate and Postdoctoral Studies for acceptance, the thesis entitled:

Targeting TSLP: Novel Therapeutics for the Treatment of Atopic Dermatitis

Submitted by Leah Mappalakayil in partial fulfillment of the requirements for

the degree of Master of Science

in Pharmaceutical Sciences

Examining Committee:

Dr. Sarah Hedtrich, Associate Professor, Pharmaceutical Sciences, UBC
Co-supervisor

Dr. Brent Page, Assistant Professor, Pharmaceutical Sciences, UBC
Co-Supervisor

Dr. Adam Frankel, Associate Professor, Pharmaceutical Sciences, UBC
Supervisory Committee Member

Dr. David Granville, Professor, Pathology and Laboratory Medicine, UBC
Supervisory Committee Member

Dr. Simon Wisnovsky, Assistant Professor, Pharmaceutical Sciences, UBC
Supervisory Committee Member

Dr. Bastien Castagner, Associate Professor, Pharmacology, McGill
Additional Examiner

ABSTRACT

Atopic dermatitis (AD) is the most common inflammatory skin disease worldwide and is characterized by intense itching and inflamed skin. Although the pathophysiology of AD is not entirely understood, key components of the relevant pathways have been identified as promising therapeutic targets. Specifically, thymic stromal lymphopoietin (TSLP) is a cytokine that acts as a master regulator of these T helper type 2 cell mediated inflammatory diseases. TSLP is involved in many different pathways that end with the activation of immune cells and the release of inflammatory mediators called cytokines.

Current first-line treatments for AD, corticosteroids and calcineurin inhibitors, are generally effective for mild to moderate cases. Issues arise in using these treatments for chronic moderate to severe cases, like adverse effects from prolonged application as well as the necessity of systemic immunosuppressants, which are not recommended for long-term use. Therefore, there has been a recent push for novel therapeutics. Inhibition of the TSLP signalling pathway has shown therapeutic potential, establishing it as a target for the treatment of atopic diseases. Injectable monoclonal antibodies that target components of the TSLP signalling pathway have been evaluated in clinical trials, some of which have reached FDA approval while others have missed primary endpoints in phase II clinical trials. However, topical administration is favourable because of the potential for reduced systemic effects and higher treatment acceptance, highlighting the need for a topically applied treatment that targets the pathophysiology of AD.

Peptide-based drugs are a growing class of therapeutics that use short amino acid chains to modulate the activity of their biological targets. One potential advantage of peptide-based therapeutics is their application as potential inhibitors of protein-protein interactions (PPIs). By designing peptides to be similar to their endogenous interacting sequence, they can serve as a starting point for the development of potent inhibitors of PPIs. Within this project, I aim to explore the druggability of the TSLP-TSLPR-Il7Rα complex by designing peptides based on relevant interaction sites and assessing these peptides alongside small molecule inhibitors for their anti-inflammatory effects. The resulting lead compounds may serve as starting points for the development of novel topical therapeutics for the treatment of AD.

LAY SUMMARY

Atopic dermatitis (AD) is a common skin disease that is associated with intense itching and inflamed skin. Often, this condition is the start of a process known as the atopic march, in which AD progresses to other allergic diseases. Because current topical treatments are not always effective for moderate to severe cases of the disease, it is important to develop therapeutics that target key players in the initiation and exacerbation of AD. Thymic stromal lymphopoietin (TSLP) and its receptors are key components of AD. Here, we aim to investigate if these components can be targeted by developing peptide inhibitors as well as assessing both peptide and small molecule inhibitors of the proteins. The resulting lead compounds may serve as a starting point in the development of therapeutics for the treatment of AD and the prevention of its progression to other allergic diseases.

PREFACE

The peptide inhibitors of TSLP signalling were based on two peptides designed and evaluated by Dr. Brent Page, Dr. Temi Idowu, and Dr. Partho Adhikary. The small molecule inhibitors, BP79 and BP75, were designed and characterized by Dr. Brent Page, Dr. Sarah Hedtrich, Dr. Temi Idowu, and Dr. Partho Adhikary. The BP79 analogues were synthesized by Christopher Hoang.

Under the guidance of Drs. Sarah Hedtrich, Brent Page, and Partho Adhikary, I took the lead in the project detailed in Chapters 3 and 4, where I was responsible for data collection and analysis. The work reported was covered by UBC Ethics Certificates #H19-03096 and #H19-00446.

The keratinocyte and fibroblast MTT assay, the skin absorption assay, and the BP79 analogue ELISAs performed by Leah Mappalakayil are included in the following submitted manuscript. Dr. Partho Adhikary was the lead investigator, responsible for the majority of data collection and manuscript composition. Dr. Temi Idowu, Zheng Tan, Christopher Hoang, Malti Dumbani, January Weiner, Dieter Beule, and Gerhard Wolber were involved in data collection and manuscript edits. Drs. Sarah Hedtrich and Brent Page were the supervisory authors on this project and were involved throughout manuscript writing and editing.

Adhikary, P. P., Idowu, T., Tan, Z., Hoang, C., Dumbani, M., Mappalakayil, L., Weiner, J., Beule, D., Wolber, G., Page, B. D. G., & Hedtrich , S. (n.d.). *Disrupting TSLP – TSLP Receptor Interactions via Small Molecule Inhibitors Yields a Novel and Efficient Treatment Option for Atopic Diseases*.

TABLE OF CONTENTS

LIST OF TABLES

LIST OF FIGURES

LIST OF ABBREVIATIONS

AD - Atopic Dermatitis

ANOVA - Analysis of Variance

Arg - Arginine

Asn - Asparagine

CD - Cluster of Differentiation

COX - Cyclooxygenase

Cys - Cysteine

DMSO - Dimethylsulfoxide

ELISA - Enzyme Linked Immunoabsorbant Assay

FBS - Fetal Bovine Serum

FDA - Food and Drug Administration

FcεRI - High Affinity IgE Receptor

FLG - Filaggrin

GM-CSF - Granulocyte-Macrophage Colony-Stimulating Factor

Glu - Glutamic Acid

h - hours

HMC - Major Histocompatibility Complex

Il - Interleukin

INFγ - Interferon Gamma

JAK - Janus Kinase

kDa - Kilodalton

Leu - Leucine

logP – Log_{10} of the Octanol-Water Partition Coefficient

Lys - Lysine

MDC - Macrophage Derived Chemokine

MTT - Thiazolyl Blue Tetrazolium Bromide

NADPH - Nicotinamide Adenine Dinucleotide Phosphate Hydrogen

NCA - No C-terminal Amidation

NF-κB - Nuclear Factor-κ-Light Chain Enhancer of Activated B Cells

NFAT - Nuclear Factor of Activated T cells

NNA - No N-terminal Acetylation

NTM - No Terminal Modifications

PBD - Protein Data Bank

PBS - Phosphate Buffered Saline

Phe - Phenylalanine

PI - Phorbol 12-Myristate 13-Acetate and Ionomycin

PMA - Phorbol 12-Myristate 13-Acetate

RANTES - Regulated Upon Activation, Normal T Cell Expressed and Secreted

S. *aureus* - *Staphylococcus aureus*

SEM - Standard Error of the Mean

Ser - Serine

STAT - Signal Transducer and Activator of Transcription

Th1 - T Helper Type 1 Cell

Th2 - T Helper Type 2 Cell

Th17 - T Helper Type 17 Cell

Thr - Threonine

TARC - Thymus and Activation-Regulated Chemokine

Tfh - Follicular Helper T Cell

Treg - Regulatory T Cell

Tr1 - Type 1 Regulatory T Cell

TSLP - Thymic Stromal Lymphopoietin

TSLPR - Thymic Stromal Lymphopoietin Receptor

Tyr - Tyrosine

VEGF - Vascular Endothelial Growth Factor

ACKNOWLEDGEMENTS

I’d like to express my gratitude to my supervisors Drs. Sarah Hedtrich and Brent Page for their invaluable guidance throughout my master's program. My committee members Dr. Adam Frankel, Dr. Simon Wisnovsky, and Dr. David Granville, as well as my chair Dr. Cory Nislow were extremely valuable to my research and the progression of my project. I’d also like to thank Dr. Partho Adhikary for training me on most of the methods used for my research. The collective knowledge of my fellow lab members was also indispensable. Additionally, the supportive and collaborative environment fostered by the graduate student community at the Faculty of Pharmaceutical Sciences has been a constant source of motivation for me. Finally, I am deeply grateful to my friends and family beyond the faculty for their unwavering support throughout the highs and lows of this journey.

CHAPTER 1. Introduction to Atopic Dermatitis, Atopic Diseases and their Therapeutics

Atopic Dermatitis

Atopic dermatitis (AD) is a common and chronic inflammatory skin disease that is characterized by intense itching and inflamed skin. Currently, 20 % of children and 1-3 % of adults are affected[1]. The impact on the quality of life of families with children with AD has been found to be comparable to those with diabetes and cystic fibrosis[2]. Additionally, the economic burden on the Canadian healthcare system is high, costing $1.4 billion per year[3]. Further exacerbation of these issues is a consequence of the atopic march, which refers to the progression of atopic diseases from AD to food allergy, allergic asthma, and allergic rhinitis[4]. Over 60 % of children with moderate to severe AD also develop allergic asthma, while about 30 % also develop food allergies.[4] These factors highlight the necessity of safe and effective treatments for AD.

Atopic Dermatitis Pathophysiology

The pathophysiology of AD involves the interplay between a variety of factors including genetics, the environment, a dysregulated immune response, and skin barrier defects (Fig 1). The two leading hypotheses concerning the initiation of AD are the “outside-inside” hypothesis, in which the disease is driven by skin barrier defects, and the “inside-outside” hypothesis, which suggests that the disease starts with an immune response to irritants and allergens[5].

The skin is the body's first line of protection against the external environment, highlighting the importance of maintaining the integrity of the skin barrier. The top layer of skin is called the

epidermis, which itself is divided into the deepest layer called the stratum basale, followed by the stratum spinosum, stratum granulosum, and stratum corneum[6]. The primary cell type in the epidermis is keratinocytes, which are produced by stem cells in the deepest layer and differentiate as they are pushed to the more superficial layers[7].

The outside-in hypothesis suggests that skin barrier defects caused by mutations in barrier proteins and exposure to environmental factors result in an immune response that causes AD[5]. As they move through the layers of the epidermis, keratinocytes undergo keratinization, a process in which a network of keratin filament and other proteins like filaggrin (FLG) form an efficient barrier between the body and the external environment[8]. FLG is released as a precursor from keratohyalin granules in keratinocytes in the stratum granulosum[9]. After these FLG monomers are dephosphorylated and cleaved, they cause the aggregation of keratin filaments[9]. Eventually, the keratinocytes undergo cell death and become primarily composed of these keratin filaments, resulting in a layer of hardened cells at the surface of the skin. Because FLG is necessary for the unique terminal differentiation of keratinocytes, mutations in this protein compromise the skin barrier. Specifically, the impaired synthesis of FLG can lead to an increase in transepidermal water loss, higher pH, and alterations in the composition of the lipids involved in the stratum corneum[10]. FLG mutations are associated with the early onset and severe presentation of AD. Other genetic components include mutations in tight junction proteins and epigenetic modifications of genes involved in skin barrier integrity[11]. However, it is important to note that the presence of these genetic mutations does not necessarily result in AD and AD can develop without these mutations.

Keratinocytes have pattern recognition receptors called toll-like receptors (TLRs), that bind to pathogen-associated molecular patterns from microbes[12]. Specific polymorphisms of TLR1, TLR6, TLR10, and genetic variations of TLR2 have been associated with AD by increasing susceptibility to *Staphylococcus aureus* (*S. aureus*), which produce proteases that disrupt the stratum corneum[13]. In AD patients, the diversity of commensal bacteria on the skin is decreased, and there is a shift towards pathogenic microbes. A decrease in FLG, higher pH levels, and a decrease in antimicrobial peptide formation promotes *S. aureus* colonization.

The inside-out hypothesis suggests that the skin barrier defects indicative of AD are caused by a dysregulated immune response. The type-2-cell-mediated immune response is usually reserved for parasitic infections; however, it is a hallmark of atopic diseases[14]. The inflammatory cytokines interleukin (Il)-4 and -2 promote the polarization of CD4+ T cells into T helper 2 (Th2) cells, which produce the cytokines Il-13, Il-4, Il-5, and Il-9[15, 16]. Il-13 is highly expressed in patients with AD, in both lesioned and non-lesioned skin[17]. High expression of Il-13 has been correlated to higher severity of AD, characterizing it as a target in AD therapeutics[17]. It is responsible for many of the symptoms classically associated with atopic diseases by causing smooth muscle hyperactivity, goblet cell metaplasia, and increased mucus secretion[18]. Il-13 has a major role in promoting skin barrier dysfunction. Mitamura *et al.* demonstrated that Il-13 upregulates keratinocyte production of periostin, which in turn downregulates FLG expression[19, 20]. Periostin is an extracellular matrix protein that interacts with sensory neurons through integrins to induce the characteristic itch that is associated with AD[21]. Therefore, Il-13 promotes epidermal barrier dysfunction by affecting proteins integral to the structural integrity of the epidermis and by promoting an itching sensation that causes patients to further damage their skin

barrier. In addition to Il-13, Il-4 is integral to the pathophysiology of AD. Along with Il-13, Il-4 promotes the downregulation of FLG, contributing to epidermal barrier defects[22]. Il-4 also regulates lymphocyte function through its action on B cells and T cells. It is involved in the isotype class switching of B cells to produce IgE, which is an antibody involved in the allergic response through binding with its high-affinity receptor FcεRI on mast cells, basophils, Langerhans cells, and dendritic cells[23, 24]. Furthermore, Il-4 can act on CD4+ T cells themselves to promote polarization to Th2 cells.

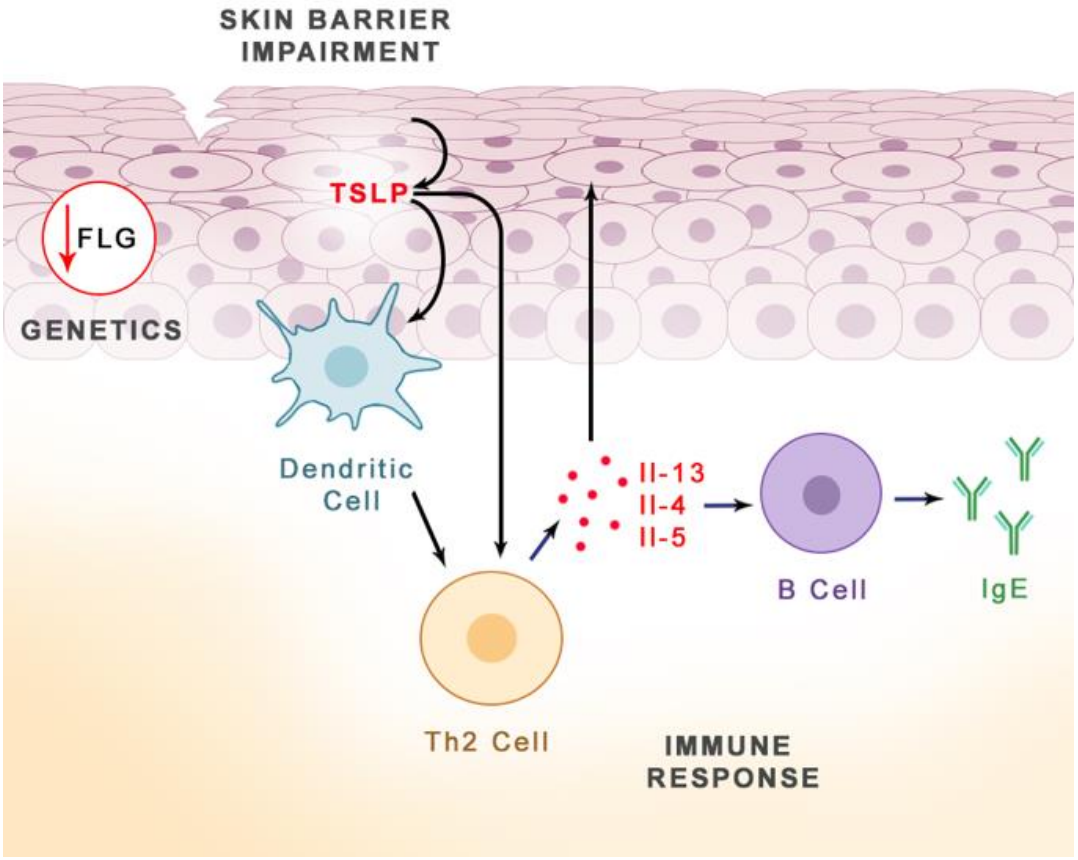

Figure 1.1 Pathophysiology of Atopic Dermatitis. Interplay between three main factors contribute to the establishment and progression of AD. Genetic factors such as FLG mutations results in impairment of the skin barrier. This causes keratinocytes to release TSLP, which promotes the type 2 immune response. The resulting cytokines and antibodies cause further skin barrier impairment and symptoms of atopy.

The Role of Thymic Stromal Lymphopoietin in Atopic Dermatitis

The pathophysiology of AD cannot be consistently defined using either of the aforementioned hypotheses, but instead a combination of the two. Because of its complexity, it is difficult to identify a molecular therapeutic target that universally contributes to the initiation and progression of AD. One consistent factor in AD is the presence of a Th2 immune response, of which TSLP is a master regulator[25]. As such, this inflammatory cytokine provides a unique target for AD therapies.

TSLP exerts its activity through the formation of the ternary complex composed of TSLP, TSLPR, and IL7Rα. Firstly, TSLP binds to TSLPR with high affinity (K_D = 32 nM). This allows IL7Rα to be recruited to the complex (K_D = 29 nM). Without the formation of the initial complex, IL7Rα and TSLPR have a low binding affinity (K_D = 20 μM)[26]. The complete assembly of the complex triggers the JAK/STAT pathway, which differs slightly based on cell type[27].

TSLP is produced by a variety of cells including activated lung and intestinal epithelial cells, keratinocytes, fibroblasts, as well as dendritic cells and mast cells to a lesser degree[28]. One of the primary cell types of interest in AD is keratinocytes. Upon skin barrier perturbation by environmental factors such as allergens or internal factors such as protein mutations and inflammatory cytokines, TSLP production by keratinocytes is initiated[29]. Although the mechanisms underlying the production of TSLP have not been fully elucidated, expression is increased by pathogenic and mechanical stimuli, including exposure to viruses, bacteria, parasites, and Toll-like Receptor agonists, as well as factors that impair the skin barrier[30]. Zhang

et al. found that human airway epithelial cells increase the expression of TSLP when exposed to peptidoglycans from gram-positive bacteria like *S. aureus*, likely through binding with a TLR[31]. TSLP expression was also increased after airway epithelial cells were exposed to the cytokines Il-13 and Il-4, which are the primary cytokines in the Th2 immune response[32]. A decrease in functional FLG protein has been associated with an increase in TSLP expression[33]. Lee *et al.* found that FLG knockdown in a keratinocyte cell line caused an increase in TSLP after stimulation with a TLR agonist[34]. Moniaga *et al.* found that FLG-deficient mice showed increased levels of TSLP mRNA and protein[35]. Using keratinocytes isolated from FLG-deficient mice, they demonstrated that the PAR-2 activation of TSLP production in keratinocytes is enhanced under FLG-deficient conditions[35].

TSLP can bind to its receptors on multiple cell types, including keratinocytes, dendritic cells, CD4+ T cells, ILC2 cells, and a variety of other immune cells[36]. TSLP can act on keratinocytes in an autocrine manner to modify gene expression (Fig 2A). It triggers STAT3 phosphorylation, which then dimerizes and translocates to the nucleus to decrease the expression of proteins such as FLG. Although a precise mechanistic understanding of this pathway remains elusive, a case can be made for a TSLP autocrine loop in keratinocytes, in which TSLP acts on keratinocytes to activate STAT3, causing the downregulation of FLG, resulting in further production of TSLP. TSLP can also activate dendritic cells[37]. Soumelis *et al.* found that TSLP activation of dendritic cells results in three things that contribute to a strong Th2 response[38]. Firstly, TSLP-stimulated dendritic cells cause a strong proliferation of CD4+ T cells compared to other stimulation methods by upregulating the production of CD40 on the surface of the cells. Secondly, these dendritic cells produce TARC and MDC, which are chemokines that attract Th2 cells. Lastly,

these dendritic cells cause the production of Th2 specific cytokines in CD4+ T cells, specifically, Il-13, Il-4 and Il-5, while inhibiting the production of the anti-inflammatory cytokine Il-10 and the Th1 cytokine INFγ. These three findings suggest that TSLP-stimulated dendritic cells prime CD4+ T cells for Th2 polarization. In AD patients, TSLP produced by keratinocytes stimulates dendritic cells within the epithelium, which then attract and stimulate Th2 production of cytokines or travel to the lymph nodes where they activate and polarize CD4+ T cells to Th2 cells[30]. TSLP can also act directly on CD4+ T cells to polarize them to effector cells that produce Il-13, Il-4, and Il-5 (Fig 2B). Rochmen *et al.* found that TSLP activates CD4+ T cells via two separate pathways[39]. Firstly, binding of TSLP to its receptor activates that JAK2/STAT5 pathway, leading to phosphorylated STAT5 translocating to the nucleus and increasing the expression of Th2-associated genes such as Il-13 and Il-4. Secondly, TSLP seems to inhibit the expression of BCL6, which is a protein that represses transcription of Il-13, Il-4, and Il-9. BCL6 expression was not affected by inhibition of the JAK2/STAT5 pathway using 50 μM of JAK2 Inhibitor II, suggesting that its inhibition proceeds via an independent mechanism. Additionally, stimulation of the production of Il-4 by T cells initiates a positive feedback loop in which Il-4 increases the expression of Il-4 receptors on the surface of other T cells, further differentiating them to Th2 cells[40]. Continuous expression of Il-13 and Il-4 causes a decrease in the expression of FLG in keratinocytes, further exacerbating skin barrier deficiencies.

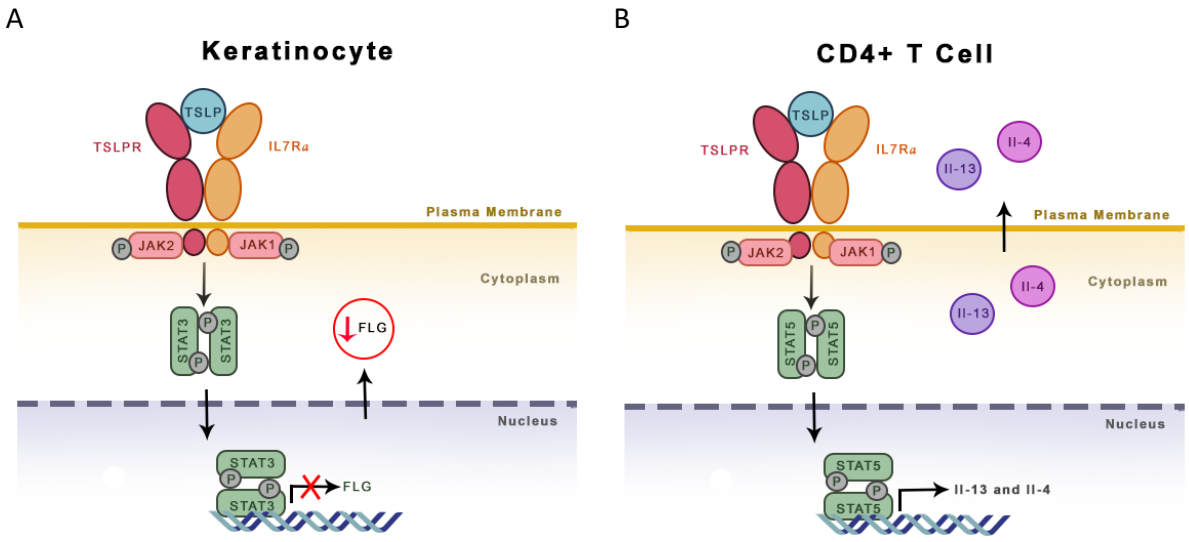

Figure 1.2 TSLP signalling pathway in Keratinocytes and CD4+ T Cells. After ternary complex formation, JAK1/2 associated with TSLPR and IL7Rα are phosphorylated. This interaction causes phosphorylation and dimerization of STAT3 in keratinocytes and STAT5 in CD4+ T cells. The activated STATs translocate to the nucleus where they regulate gene expression to decrease FLG expression in **(A)** keratinocytes and increase Il-13 and Il-4 expression in **(B)** CD4+ T cells.

The Atopic March

The atopic march refers to the temporal progression of specific atopic diseases. According to cross-sectional and longitudinal studies, the presentation of atopic diseases usually begins with AD in early childhood and then develops into food allergy and eventually allergic asthma and allergic rhinitis[4]. Allergic asthma is characterized by inflammation and remodelling of the airways while allergic rhinitis exhibits similar symptoms in the nasal mucosa[41]. AD, food allergy allergic asthma, and allergic rhinitis can gradually resolve with age or can become chronic, spanning many years[42]. Despite this information, treatments that target the atopic march are limited, likely due to an incomplete understanding of its pathophysiology. One possible mechanism begins with the skin barrier dysfunction that leads to AD[4]. Once the Th2 immune

response has been established, the associated cytokines, including TSLP, may travel to the gastrointestinal tract and respiratory tract to initiate food allergy, allergic asthma, and allergic rhinitis[42]. Although there are likely many other pathways involved in the atopic march, TSLP seems to be a key player. Many studies have elucidated a link between the development of AD and the eventual progression to food allergy, allergic asthma, or allergic rhinitis through TSLP signalling[43–45]. For example, Zhang *et al.* used mouse models to demonstrate that TSLP over-expression in keratinocytes exacerbated symptoms of experimentally established asthma[46]. Similarly, Noti *et al.* found that exposure to food allergens through the skin can induce food allergy through TSLP signalling[47]. Because the atopic march can cause disease in many organ systems, it is important to target it therapeutically in early stages when it presents as AD. This distinguishes AD from the other atopic diseases as an important stage for therapeutic intervention.

Current Therapeutics for Atopic Dermatitis

The first-line treatments for AD are topical corticosteroids and calcineurin-inhibitors[48]. Because of the multiple potencies of corticosteroids available, it can be prescribed for varying severities of AD. Topical corticosteroids tends to be very effective at treating mild to moderate AD with minimal side effects. If the disease is more severe or the patient presents with lesions in areas with thin skin such as the eyelids, calcineurin inhibitors like pimecrolimus and tacrolimus are utilized[49]. However, they are associated with a higher frequency of adverse effects like burning and pruritis. Treatment becomes even more complicated in severe chronic cases. Long term use of highly potent topical steroids are associated with skin atrophy, rosacea, perioral dermatitis, and purpura[50]. In cases where topical treatments are ineffective, patients can be prescribed

systemic glucocorticoids; however, these drugs are not recommended for prolonged use[51]. The ineffectiveness of the first line therapies in moderate to severe cases of AD shows that there is an unmet medical need for new therapeutics.

As the pathophysiology of AD becomes more clearly understood, components of the signalling pathways involved emerge as potential therapeutic targets. Small molecule JAK inhibitors have been developed for the treatment of a variety of immune related disorders[52]. For example, upadacitinib is an orally-administered JAK1 inhibitor that has been approved for the treatment of moderate to severe rheumatoid arthritis and atopic dermatitis[53]. The possibility of serious side effects like thrombosis has prevented this drug from being prescribed as an initial treatment. Baricitinib is an orally-administered JAK1/2 inhibitor that has FDA approval for the treatment of rheumatoid arthritis and has successfully passed phase III clinical trials for the treatment of AD[54]. Tofacitinib is a JAK1/3 inhibitor that has been approved by the FDA as an oral treatment for different types of arthritis and ulcerative colitis[55]. Similar to other JAK inhibitors, it is associated with cardiovascular adverse events like thromboembolisms, which has prompted the FDA to add a boxed warning to the tofacitinib label[56]. Recently, it has been reformulated for topical application and has completed phase II clinical trials for the treatment of AD[57]. The JAK inhibitors that have been developed show promising efficacy in clinical trials. Thus, targeting the JAK/STAT pathway can be advantageous as a single drug can be used for multiple immune disorders as described above. However, it may also result in more adverse effects because of its pleiotropic nature.

In addition to small molecules, biologics are being developed as novel therapeutics for the treatment of AD. Because the Th2 immune response is a ubiquitous characteristic of AD, many monoclonal antibodies that target its components have been developed and undergone clinical trials. Dupilumab was the first biologic to gain FDA approval for the treatment of AD[58]. It is a humanized monoclonal antibody that binds to Il-R4α, a receptor chain that is part of the IL4Rα-γ receptor complex that binds Il-4 as well as the Il-4Rα-Il-13α1 receptor complex that binds both Il-4 and Il-13. By blocking this receptor chain, dupilumab inhibits both Il-13 and Il-4 signalling, affecting both CD4+ T cells and keratinocytes. It has been approved by the FDA for the treatment of AD in adults. Lebrikizumab is another humanized monoclonal antibody that targets Il-13 signalling by directly binding to the interleukin to inhibit its interaction with its receptor[59]. It has successfully passed phase III clinical trials[59]. As AD can also involve Th17 and Th1 immune responses, antibodies against Il-22 and Il-17A have also been developed and tested in clinical trials[60, 61].

Tezepelumab is a human monoclonal antibody that targets TSLP to inhibit its binding to its receptor complex. It has successfully passed phase III clinical trials for the treatment of severe asthma but failed to reach its primary endpoints in a phase II clinical trial for the treatment of AD[62, 63]. Although they have the potential to be effective treatments for AD, antibodies like tezepelumab require subcutaneous injection, which may be an unfavourable route of administration. Currently, there are no clinically approved topical small molecule or peptide inhibitors of TSLP and its receptor complex.

Peptides vs Small Molecule Therapeutics

The topography of PPIs like in the TSLP-TSLPR-Il7Rα complex makes them a notoriously difficult target for small molecules, as they often lack deep lipophilic grooves and instead have spread out hotspots (*vide infra*). Small molecules often target deep pockets on the protein surface that interact with a ligand or substrate. By mimicking the ligand interactions, these small molecule inhibitors are able to bind tightly to these pockets. In comparison, inhibitor binding sites for PPIs are shallower and cover larger surface areas. A feature of PPIs that enhances their druggability is hotspots, which refer to a few amino acids that form key interacting regions across the interacting surfaces that are essential for high-affinity binding[64]. Because these hotspots can be far from each other, it is difficult for a small molecule to target more than one of these essential regions. In comparison, peptides can be designed to be larger or less linear than traditional small molecules, allowing them to interact with multiple regions of the PPI[65]. This can be done through modifications that maintain the secondary structure of the peptides such as hydrocarbon staples or cyclization[65,66].

Although some peptides that are the same as their endogenous counterparts exist as therapeutics, like insulin and adrenocorticotropic hormone, they must often undergo modifications to make them more drug-like[67]. This requirement is based on these facts: they are associated with predictably bad pharmacokinetics, specifically poor bioavailability, quick metabolism by proteases, and rapid renal clearance[68]. The size of peptides usually falls between that of small molecules (<500Da) and biologics (>5000Da). Molecular weight along with other physiochemical properties such as logP may result in low oral bioavailability and membrane permeability[69]. If ingested, they are prone to degradation in the digestive tract by stomach acid

and digestive enzymes that normally degrade proteins[68]. If the peptide remains intact after oral administration, crossing from the intestine to the bloodstream remains a hurdle. Similarly, topically applied peptides are not predicted to cross the skin barrier[70]. In addition to poor biodistribution, peptides are quickly metabolized in the body, minimizing their half-life. This rapid metabolism is due to the prevalence of tissue proteases that degrade peptides and proteins.

By altering the initial peptides to be more drug-like, these compounds can be transformed into peptidomimetics that fall into four categories depending on the extent of modification[71]. Class A mimetics refer to peptides that are structurally very similar to their endogenous counterpart. They include natural peptides including insulin and cyclosporin, as well as peptides with slight modifications like hydrocarbon staples[72,73]. Class B mimetics have more modifications such as the addition of non-natural amino acids and backbone alterations that prevent recognition by proteases to hinder metabolism[74]. Methods to increase membrane permeability like cyclization and N-methylation can also be employed[75]. Class C mimetics are extensively modified to have more small molecule properties, with the complete alteration of the backbone and the inclusion of chemical moieties mimicking key residues from the original peptide. Class D mimetics are small molecules that retain the bioactivity of the original peptide while having minimal structural similarities. Through this process, peptides based on endogenous sequences involved in PPIs can be used as a starting point in the drug development process to target large and flat protein surfaces that are difficult for small molecules to interact with.

Objective & Hypothesis

The TSLP signalling pathway presents an attractive target for the treatment of AD because of the extensive involvement of this cytokine in the pathophysiology of the disease. The druggability of TSLPR-TSLP-IL7Rα can be explored using peptides and small molecules designed to inhibit ternary complex formation. Peptides based on the regions of TSLP and IL7Rα that interact with TSLPR may interact with the receptor complex in a similar manner as the endogenous sequences to potently inhibit TSLPR signalling in keratinocytes and CD4+ T cells. These will be developed and evaluated for their biological activity. Small molecules developed by the Page Laboratory will be evaluated as inhibitors of TSLP signalling. We hypothesize that peptides and small molecules designed to inhibit ternary complex formation will characterize TSLPR as a druggable target. The resulting inhibitors may serve as the starting point for the development of topical therapeutics for AD and prevention of the atopic march.

Overall Aim: Design and evaluate the anti-inflammatory effect of peptide inhibitors, as well as assess small molecule inhibitors of TSLP signalling

Developing and Evaluating Peptide Inhibitors of TSLP Signalling

Specific Aims

1) Design peptides that inhibit the interaction between TSLP and its receptor complex.
2) Screen and assess the anti-inflammatory activity of the peptide inhibitors
3) Assess the biocompatibility of the peptide inhibitors

Evaluating Small Molecule Inhibitors of TSLP Signalling

Specific Aims

1) Further characterize the previously developed small molecule inhibitor, BP79
2) Screen and assess the anti-inflammatory activity of novel small molecule inhibitors

CHAPTER 2. Materials and Methods for Evaluating Potential Inhibitors of TSLP Signaling in AD

Docking

The co-crystal structure of IL7Rα-TSLP-TSLPR (PDB: 511J) was imported to PyMol and a separate selection of chain C which corresponds to TSLPR, was created. The structure was imported into Maestro (Schrödinger) and prepared for docking using the Protein Preparation function. Grid-based constraints were created by analyzing the co-crystal structure of TSLPR-TSLP-IL7Rα in PyMol and determining the relevant interactions. The four TSLPR residues that were selected for potential hydrogen bond constraints were Ser110, Trp112, Arg111, and Tyr96. The locations of three TSLP residues were selected for potential positional constraints, including Glu62, Phe63, and Asn64. Finally, the core atoms selected for the potential core pattern comparison were select side chains and backbone carbon atoms in Phe63 to Val67 of the TSLP-P4-fragment. A combination of these constraints were used to dock the P4-modified peptides and the P4 alanine scan peptides to TSLPR. Ligands were prepared for docking using the LigPrep which retained the chiral centers and the ligands states generated at a pH of 7.0 ± 2. The sequence of TSLP that corresponds to the peptide P4 (aa60-69) was imported from PyMol to Maestro. Modification of the terminal functional groups was done using the 2D builder function in Maestro to add an acetyl group to the N-terminal and an amide to the C terminal in order to yield the P4-modified peptides. Additionally, the side chain of Glu63 was added back into the sequence as it did not appear in the crystal structure. The resulting peptides were prepared for docking using the LigPrep function. The resulting ligands were then docked using GLIDE (Maestro) and with a combination of the grid constraints and the core pattern comparison

previously mentioned. Standard precision was used and Epik state penalties were added to the docking scores. The latter was added to favour probable ionization states during docking[76].

Cell culture

HUT78 cells (male, T cell) were obtained from the American Type Culture Collection (ATCC). They were cultured in RPMI-1640 Medium (Sigma Aldrich, Oakville CA, Cat# R8758) supplemented with 10% (v/v) of FBS (Sigma Aldrich, Oakville CA, Cat# F1051) and 1% (v/v) of Penicillin-Streptomycin (Sigma Aldrich, Oakville CA, Cat# P4333), with media changes every three days. Before using in an experiment, the cells were washed with PBS and allowed to proliferate in culture for one day.

Primary human CD4+ T cells were isolated from blood donor buffy coats (CREB approval 2019.023). Peripheral blood mononucleocytes (PBMCs) were isolated from the buffy coats using Lymphoprep density gradient medium (STEMCELL, Vancouver CA, Cat # 07851) and CD4+ T cells were isolated from the resulting PBMCs using the EasySep Human CD4+ T cell Isolation Kit (STEMCELL, Vancouver CA, Cat# 17912). The CD4+ T cells were cultured in RPMI-1640 Medium, with media changes every three days.

Primary human keratinocytes and fibroblasts were isolated from donor foreskin and belly skin (CREB approval #H19-03096). Keratinocytes were cultured in EpiLife medium (Gibco; Thermo Fisher Scientific, Cat# MEPI500CA) supplemented with Human Keratinocyte Growth Supplement (Gibco; Thermo Fisher Scientific, Cat# S0015). Fibroblasts were cultured in DMEM – high glucose (Sigma Aldrich, Oakville CA, Cat# D6429) supplemented with 10% (v/v) of FBS

(Sigma Aldrich, Oakville CA, Cat# F1051) and 1% (v/v) of Penicillin-Streptomycin (Sigma Aldrich, Oakville CA, Cat# P4333). Media was changed every three days for both cell types.

Chemical Compounds

The small molecules were synthesized by the Page Laboratory. BP79 was first discovered through a hit expansion process where different chemical structures were modified on the hit scaffold originally identified (C7 and C13). The structure of BP79 includes a substituted phenyl ring attached to a core composed of an internal amide and an alkene, which is connected to a terminal amide tail. Different chemical modifications were made to the terminal amide of BP79 to explore how these changes would affect biological activity, leading to a series of BP79 analogues. The structure of the compounds were characterized by ^{1}H-NMR and ^{13}C-NMR and the masses were determined by LC/MS. These analogues were tested for purity by LC/MS and all of them showed greater than 95 %, with the exception of BP254, and BP287.

The initial five peptides and the P4-modified peptides were produced using solid phase peptide synthesis by Biomatik. All peptides were TFA salts and had a purity of over 95 % as determined by High-Performance Liquid Chromatography.

HUT78, CD4+ T Cell, and Keratinocyte Enzyme Linked Immunosorbent Assay

The Enzyme Linked Immunoabsorbant Assay (ELISA) uses antibodies against key components of the TSLP signalling pathway to assess inhibition by the peptides or small molecules.

HUT78 cells or primary CD4+ T cells were seeded in 24 well plates with a density of 0.5 x 10^6 cells/mL. HUT78 cells were treated with 100 ng/mL PMA, 1 μg/mL ionomycin, and 50 ng/mL TSLP (Sigma Aldrich, Oakville CA, Cat# P1585, #I0634, # SRP4896). CD4+ T cells were treated with 25 μL/million cells of ImmunoCult Human CD3/CD28 T Cell Activator (StemCell, Vancouver CA, Cat#10991) and 50 ng/mL TSLP. Keratinocytes were seeded in 24 well plates and allowed to reach ~60 % confluency before treating with 50 ng/mL TSLP. For the peptides, the cells were treated at concentrations of 200 μM, 100 μM, 50 μM, and 25μM. The initial five peptides were dissolved in Milli-Q water while the P4-modified peptides were dissolved in PBS + 0.5 % DMSO. For the small molecules, the cells were treated at concentrations of 20 μM, 10 μM, and 5 μM for the first set of experiments and 1 μM for the second. After treatment, the cells were allowed to incubate at 37 °C for 36 h, after which the samples were collected. Levels of Il-13 and Il-4 production by HUT78 cells and CD4+ T cells were determined using uncoated human Il-13 and Il-4 ELISA kits (Invitrogen; Thermo Fisher Scientific, Oakville CA, Cat# 88-7439-88, # 88-7046-88). The level of TSLP production by keratinocytes was determined using human TSLP ELISA kits (Invitrogen; Thermo Fisher Scientific, Oakville CA, Cat# 88-7497-88).

Turbidity Assay

In this assay, the precipitate formed by insoluble compounds will scatter photons, resulting in a turbidity measurement. Alternatively, absorbance can be measured as an indication of the photons absorbed by the compound. Peptides containing tyrosine and tryptophan have absorbances at 280 nm. Those that do not contain these amino acids can be detected at 205 nm[77]. Therefore, in a turbidity assay, the optical density is measured at a much higher wavelength, in this case, 600 nm.

peptides were dissolved in either PBS or PBS + 0.5 % DMSO. 300 μM, 100 μM, 33 μM, 11 μM, and 3.33 μM of each solution was loaded into a 384 well plate in duplicates. A vehicle control was used for each solvent. The plate was placed on a shaker for 15 minutes. The optical density was measured at 600 nm using the μQuant microplate spectrophotometer (BioTek Instruments, USA)

MTT Cell Viability Assay

This assay uses metabolic activity as a measure of cytotoxicity. NAPDH-dependent oxidoreductase enzymes convert Thiazolyl Blue Tetrazolium Bromide (MTT) to formazan crystals[78]. Cells that retain metabolic activity after exposure to the peptides will produce the purple formazan crystal, which is then dissolved to measure optical density.

Primary human keratinocytes (0.5 x 10^4 cells/well) and fibroblast (0.5 x 10^4 cells/well) cells were treated with either the P4-modified peptides or the small molecules at 200 μM, 100 μM, 50 μM, 25 μM, 12.5 μM, 6.25 μM, 3.13 μM, and 1.56 μM or 20 μM, 10 μM, 5 μM, 2.5 μM, 1.25 μM, 0.625 μM, and 0.313 μM respectively. The cells were then incubated for 36 h. Subsequently, the media was aspirated and 5 mg/mL MTT (Sigma Aldrich, Oakville CA, Cat# M2128) was added for 4 h for keratinocytes or 3 h for fibroblasts. DMSO was added to solubilize the formazan crystals. The absorbance was measured at 570 nm using the μQuant microplate spectrophotometer (BioTek Instruments, USA). Cell viability was determined as a percentage of the vehicle control group treated with a medium containing 0.5 % DMSO and 0.2 % DMSO for the P4-modified peptides and the small molecules respectively.

Live and Dead Cell Stain Assay

The Live and Dead Cell Stain Assay uses a mixture of two fluorescent dyes that stain live and dead cells to assess cell membrane permeability as a measure of cytotoxicity[79]. The dye used for live cells penetrates the cell membrane and enters the cytosol where it is cleaved by intracellular esterases, resulting in fluorescence. The dye used for dead cells can only enter the cells if the membrane is compromised. Once inside dead cells, it intercalates within DNA, resulting in fluorescence.

Primary human keratinocytes and fibroblasts were seeded in 96 well plates (0.25×10^4 cells/well). The next day, they were treated with 100 μM of the P4-modified peptides and incubated for 36 h. Subsequently, the media was aspirated and 100 μL of live and dead cell assay stain (Abcam, Cat# ab115347) in PBS was added at concentrations of 5 X for keratinocytes and 7 X for fibroblasts. The cells were imaged using EVOS M5000 fluorescence microscope (Thermo Scientific, USA) and semi-quantified using ImageJ. For semi-quantification, a macro was created to analyze the images and count the number of particles corresponding to both live and dead cells. This macro involved using a gaussian blur, background subtraction, adjustment of brightness and contrast, and setting a threshold to minimize noise and maximize the selection of the fluorescence signal. The resulting number of particles was then used to determine the percentage of dead cells relative to total cell count.

Skin Absorption Test

Skin permeation of BP79 was assessed using the Franz cell setup (static type, volume 12 mL, diameter 15 mm) and LC/MS. Each Franz cell body was filled with PBS and a magnetic stir bar was used to gently agitate the PBS over the course of the experiment. Excised human skin was thawed and punched disks with a diameter of 2 cm were placed onto Franz cells with the stratum corneum exposed to air and the dermis in contact with the PBS. Treatment groups included four time points for BP79 as well as DMSO as a vehicle control. 100 μL of 20 μM BP79 or DMSO was applied topically on the skin. BP79 was allowed to penetrate the skin for 2, 4, 8, and 24 h while DMSO was allowed to penetrate for 24 h. Subsequently, the skin disks were removed so that the PBS within the Franz cells could be collected. The resulting samples were stored at -20 °C and analyzed by LC/MS.

Statistical Analysis

The statistical analysis was performed using GraphPad 9.0. The standard error of the mean (SEM) was determined for all experiments. No further statistical analysis was performed on the screening experiments, which had two biological replicates. For all other experiments, the mean values of the treatments were compared to either the vehicle control or the positive control using a one-way ANOVA.

CHAPTER 3. Design and Evaluation of Peptide Inhibitors of TSLP Signalling

3.1 Initial Peptides Design

To target the interaction between TSLP and its receptor complex, the X-ray crystal structure of TSLP in complex with its receptors TSLPR and Il7Rα was used for the rational drug design of peptide inhibitors (PDB 5J11). TSLP is composed of four alpha helices named αA (aa30-56), αB (aa71-85), αC (aa96-110), and αD (aa136-152) as well as the AB loop (aa60-69) and CD loop (aa125-131). The interaction between the ternary complex is characterized by three sites, each corresponding to a different interaction interface. TSLPR interacts with TSLP via site I, Il7Rα interacts with TSLP via site II, and Il7Rα interacts with TSLPR via site III. Previously, the Page Laboratory designed two peptides (P1 and P2) based on the sequences of the AB loop and αD that interact within site I. Because these peptides stabilized TSLPR in a thermal shift assay and exhibited a dose-response after assessing for anti-inflammatory effects using an ELISA, they were used as a launch pad for further investigation (Sup 1, 2). The structure elucidated by Verstraete *et al.* was used to design other potential peptide inhibitors based on protein-protein interaction hotspots (Fig 3.1). This resulted in five initial peptides (P3, P4, P5, P6, and P7) (Table 3.1). P3 and P4 were slight variations of the initial peptides previously designed by the Page Laboratory. The origin sequence of P3 was shifted from TSLP 149-159 to TSLP 141-150. P2 was originally based on murine TSLP, so Gln64 was changed to Asn64 when designing P4.

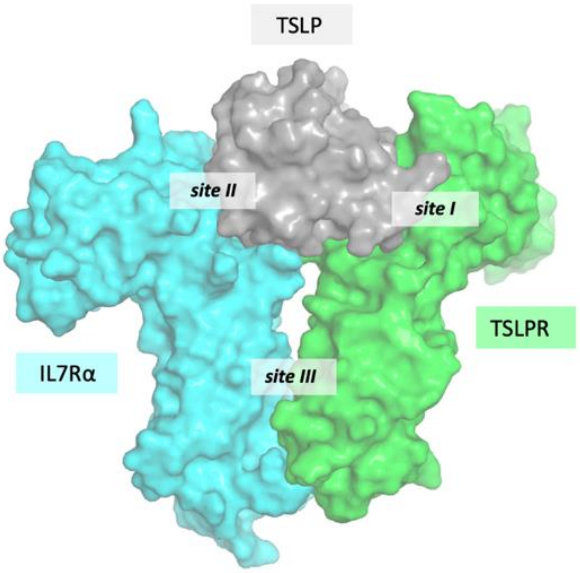

Figure 3.1 TSLP in Complex with its Heterodimeric Receptor. The surface of TSLPR is shown in green, the surface of IL7Rα is shown in cyan, and the surface of TSLP is shown in grey. The three sites of interaction within the ternary complex are shown.

Peptide Name	Origin Sequence	Secondary Structure of Origin Protein	Sequence	Molecular Weight (g/mol)	LogP
P1	hTSLP (aa149-158)	α helix	Ac-RRFNRPLLKQ-NH_2	1372.69	-20.71
P2	mTSLP (aa60-69)	α with tail	Ac- STEFQNTVSC- NH_2	1158.25	-12.39
P3	hTSLP (aa141-150)	α helix	Ac-VSQLQGLWRR-NH_2	1285.52	-13.17
P4	hTSLP (aa60-69)	α with tail	Ac-STEFNNTVSC-NH_2	1141.20	-13.94
P5	hIL7R (aa179-188)	β strand	Ac-THVNLSSTKL-NH_2	1141.32	-11.40
P6	hIL7R (aa184-193)	β strand	Ac-SSTKLTLLQR-NH_2	1189.42	-13.97
P7	hTSLP (aa40-49)	α with bend	Ac-KAAYLSTISK-NH_2	1124.35	-11.51

Table 3.1 The Origin and Physiochemical Properties of the Initial Peptides. The amino acid number in the TSLP-TSLPR-Il7Rα complex corresponds to the sequence the peptide was based on. All the peptides have terminal modifications, specifically, N terminal acetylation and C terminal amidation.

Both P3 and P4 were based on sequences of TSLP that are involved in site I, which refers to the interacting region between TSLP and TSLPR[26]. The sequence of P3 was based on αD. In the co-crystal structure, hydrogen bonds form between TSLP-Arg150 and TSLPR-Asp92, TSLP-Arg153 and both TSLPR-Asp92 and TSLPR-Tyr115, and TSLP-Arg149 and TSLPR-Tyr115. P1 was designed to include all three of these interactions and demonstrated some activity (Sup 1, 2). If the helical structure of the sequence is maintained, the resulting peptide may bind in the same manner as the original sequence. Therefore, P3 incorporated residues involved in the first two interactions as well as residues only predicted to be involved in the alpha helix formation. (Fig 3.2 A).

Apart from the four main helices, TSLP contains a flexible sequence called the AB loop that interacts with TSLPR and is connected to αA, which interacts with IL7Rα. Verstraet *et al.* described two key interactions within this site between the TSLP-Thr66 backbone carbonyl oxygen atom and the TSLPR-Tyr96 phenolic OH group as well as the TSLP-Asn65 amide and the TSLPR-Tyr115 hydroxyl group[26]. Upon inspection of the co-crystal structure using PyMol, three more potential interactions were predicted. These were between the TSLP-Asn65 backbone nitrogen and the TSLPR-Ser110 backbone carbonyl oxygen atom, the TSLP-Asn64 sidechain oxygen and both the TSLPR-Ser110 backbone nitrogen and TSLPR-Arg111 sidechain. Verstraet *et al.* found that the interaction between the AB loop and TSLPR may result in conformational changes within the TSLP protein, priming the TSLP-TSLPR complex for IL7Rα recruitment because it physically links site I to site II through its interaction with αA[26]. Therefore, P4 was designed based on the AB loop. Although TSLP-Ser60 and Thr61 were not shown to be involved in any interactions with TSLPR in the co-crystal structure, they were in close proximity to the

TSLPR-Asp197 side chain carboxylic acid and were therefore included in the sequence (Fig 2.3 B).

P5 and P6 were based on site III, which is the region of interaction between TSLPR and IL7Rα. Specifically, the Il7Rα-Arg193 sidechain interacts with TSLPR-Asp132 and TSLPR-Asp176 sidechains. Also, the side Il7Rα-Lys187 sidechain interacts with the TSLPR-Glu159 sidechain. These key residues in Il7Rα are part of two anti-parallel beta strands (aa179-193). In the design of P5 and P6, these beta strands were split into two, with an overlapping region to include the key interacting residues (Fig 3.2 C, D).

P7 was based on site II, which is the region of interaction between TSLP and IL7Rα, in which αA is a major contributor. Within the sequence of this helix, the TSLP-Ser45 sidechain interacts with the IL7Rα-Tyr159 backbone carbonyl oxygen atom and the TSLP-Lys49 backbone interacts with the Il7Rα-Ile102 backbone. P7 included all the residues involved in these interactions (Fig 4.3 E).

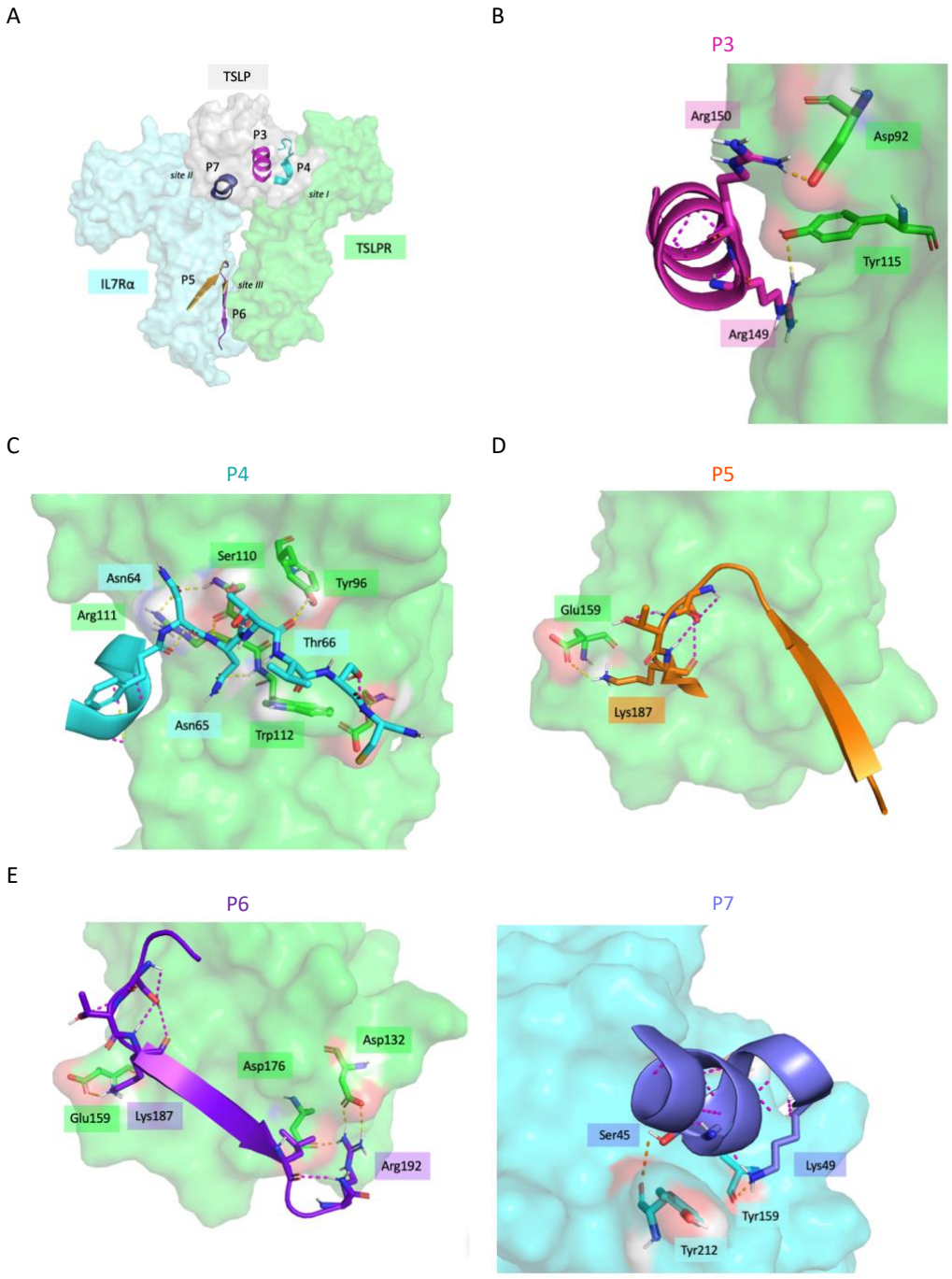

Figure 3.2 Co-crystal Structure of TSLP or Il7Rα Fragments Corresponding to the Initial Peptides. The five sequences that were used to design the five initial peptides are shown in magenta (P3), cyan (P4), orange (P5), violet (P6), and purple (P7). P3 and P4 interact within site I, P7 interacts within site II, and P5 and P6 interact within site III. The surface of TSLPR is shown in translucent green and the surface of IL7Rα is shown in translucent cyan. Hydrogen bonds between the fragment and the receptor are shown in yellow dashed lines. Orange dashed lines are used if the interaction was only defined by Verstraet et al. and not found using PyMol[26]. Intramolecular hydrogen bonds are shown in magenta dashed lines.

3.2 Initial Peptides Screening

The two target cell types for the initial five peptides are keratinocytes and CD4+ T cells as both express TSLPR and are involved in the initiation and progression of AD. To screen the initial five peptides for their activity against TSLPR, an ELISA in HUT78 cells was used. HUT78 cells are a cutaneous T lymphocyte cell line that have similar proximal TCR signalling events when compared to activated peripheral blood T cells[80]. The HUT78 cells were treated with PMA and ionomycin (PI) to stimulate general cytokine release, including Il-13 and Il-4. The cells were also treated with TSLP, which increases the expression of the Th2 cytokines Il-13 and Il-4, to emulate the immune response associated with AD. If the peptides inhibit the formation of the TSLPR-TSLP-Il7Rα ternary complex, a decrease in cytokine expression relative to the vehicle control should be observed.

In the assay, TSLP successfully increased cytokine release relative to the PI treated cells while the vehicle control had minimal effect on cytokine release. P3 and P6 exhibited a slight dose-response in Il-13 expression, but the inhibition of cytokine expression was not statistically significant. All five peptides exhibited a dose-response in Il-4 expression, with inhibition by P4 at the two highest concentrations having a statistically significant effect (Fig 2.4). At 200 μM and 100 μM, P4 brought Il-4 expression down to approximately PI treated control levels. This assay identified P4 as a promising initial hit compound as it inhibited Il-4 expression by 39% at 200 μM. However, a potentially confounding development was that P4 had poor solubility in Milli-Q water, as indicated by precipitate formation during treatment, which was further confirmed in a turbidity assay (Fig 3.8). Additionally, it was noted that a buffered vehicle would

be more appropriate and would help ensure ionizable residues (Glu63, Asn64, Asn65) were charged in solution to help with the solubility of P4.

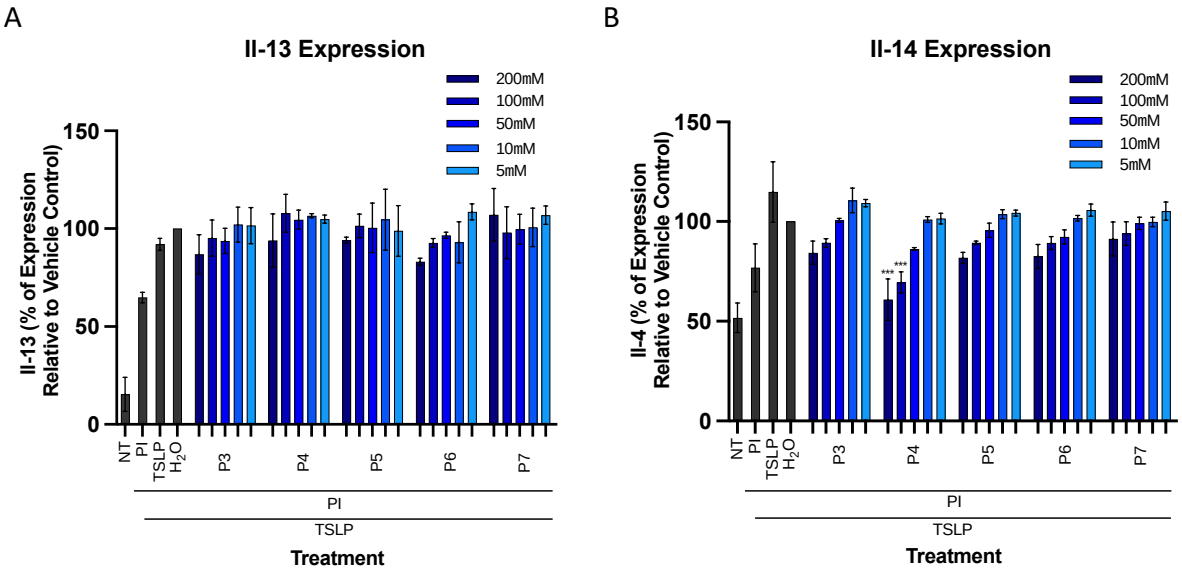

Figure 3.3 Dose Dependent Inhibition of Th2 Cytokine Release by the Initial Five Peptides in HUT78 Cells. (A) shows the effect of the five initial peptides on Il-13 expression and **(B)** shows their effect on Il-4 expression. Error bars represent the standard error of the mean. All values are represented as percent expression relative to the DMSO control. All initial five peptides were tested at 200 µM, 100 µM, 50 µM, 10 µM, and 5 µM. All values were compared to the DMSO control. *p < 0.05, **p < 0.01, ***p < 0.001, ns not indicated. (N = 3)

3.3 P4-Modified Peptide Design and Docking

To address the insolubility of P4 observed while performing the first screening ELISA, a series of modifications were made to P4. Removing the N and C terminal modifications (acetylation and amidation, respectively) was explored as a way to improve solubility. Additionally, adding charges by removing the terminal modifications may allow the peptides to make ionic interactions with TSPLR. For example, the TSLPR-Asp197 carboxylic acid may form an ionic interaction with a free N-terminal as opposed to an acetyl group. Noticing that cysteine was not

predicted to interact with TSLPR in the co-crystal structure, the impact of removing the cysteine residue from the initial sequence was explored. Altogether, these changes resulted in eight P4-modified peptides: P4, No N-terminal Amidation (NNA), No C-terminal Acetylation (NCA), No Terminal Modifications (NTM), P4', NNA', NCA', and NTM' (prime ('): no cysteine) (Table 4.2)

The P4-modified peptides were docked to TSLPR using GLIDE to assess how removing terminal modifications and the cysteine residue affects binding. The docking protocol used was based on the hypothesis that all the P4-modified peptides would interact with TSLPR similar to the manner in which the AB loop of TSLP binds to TSLPR. During the generation of the receptor grid, multiple possible grid-based constraints were made. Through analysis of the X-ray crystal structure of TSLP-TSLPR-Il7Rα (PDB:5J11) using PyMol, four TSLPR residues were selected for possible hydrogen bond constraints, including the backbone of Ser110, the backbone of Trp112, the side chain of Arg111, and the side chain of Tyr96 (Fig 3.2 B). Positional constraints restrict the location of selected ligand atoms within a chosen sphere while docking. The locations of the sidechains of TSLP-Glu62, -Phe63, and -Asn64 within the co-crystal structure were added as positional constraints. During ligand docking, core pattern comparison can be used as a constraint, in which specific residues from a reference ligand can be selected to restrict the docking of the prepared ligands. The side chains and the carbon atoms in the backbones of Phe63 to Val67 of the TSLP P4-fragment were selected as the core. Multiple combinations of these constraints were tested to dock the P4-modified peptides to TSLPR. All of the P4-modified peptides successfully docked to the orientation of the TSLP P4-fragment using the core pattern comparison and the Glu62 positional constraints (Fig 3.4).

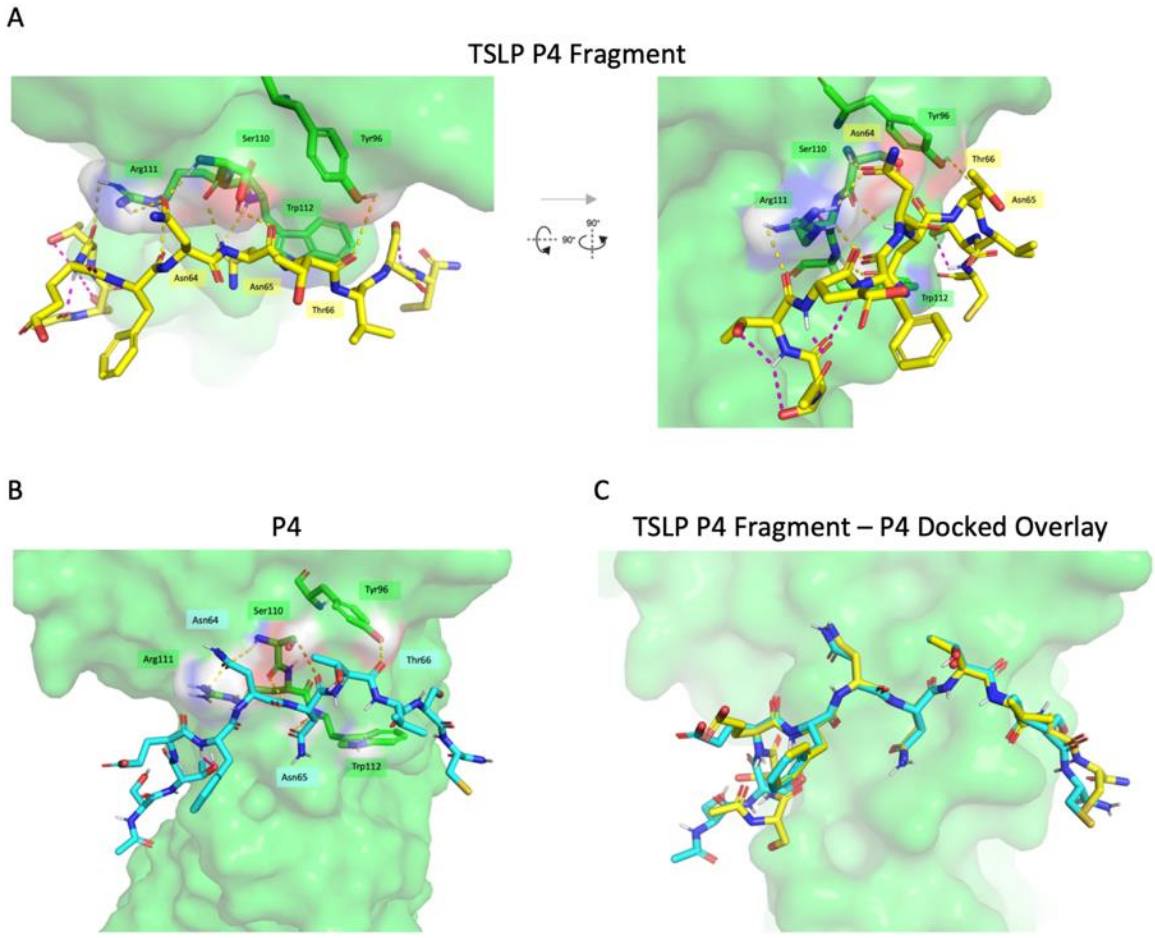

Figure 3.4 Comparison of TSLP P4-Fragment and Docked P4. (A) Two orientations of the TSLP P4-Fragement and TSLPR from the co-crystal structures are shown. **(B)** P4 docked to TSLPR is shown. The surface of TSLPR is shown in translucent green. Hydrogen bonds between the fragment and the receptor are shown in yellow dashed lines. Orange dashed lines are used if the interaction was only defined by Verstraet et al. and not found using PyMol[26]. Intramolecular hydrogen bonds are shown in magenta dashed lines. **(C)** The TSLP P4-fragment and the docked P4 peptide are overlain to show similarity in binding modality

There were eight key hydrogen bonds between the TSLP P4-fragment and TSLPR. Docked P4 retained six of these interactions while losing the interactions made by the P4-Thr61 and P4-Phe63 backbone oxygens. The rest of the P4-modified peptides also followed this pattern. With the exception of P4, all other peptides also made hydrogen bonds between TSLPR-Asp197 and Ser60 or Thr61 or both. This additional interaction may be why the docking scores for these

peptides are better than that of P4 (Table 3.2). With the exception of NNA, all peptides without N-terminal acetylations also made an ionic interaction with Asp197 through the free N-terminal. Once again, this additional interaction may be why NTM, NNA', and NTM' had better docking scores than NNA. Both NCA and NCA' made an interaction between Thr61 and TSLPR-Tyr116.

The TSLP P4-fragment had four intramolecular hydrogen bonds that helped maintain the structure of the peptide. Although all these exact hydrogen bonds were lost when docking the P4-modified peptides, P4 had a bond between the Phe63 backbone nitrogen and the Ser60 side chain that was similar to the bond between the Phe63 backbone nitrogen and the Ser60 backbone oxygen in the TSLP P4-fragment. These intramolecular hydrogen bonds were not enough to retain the helical structure of the end of the original peptide fragment. With the exception of NNA, the rest of the P4-modified peptides also have at least one intramolecular hydrogen bond involving the ends of the peptides, although none are the same as the TSLP P4-fragment. P4, P4', and NTM' all have the same intramolecular hydrogen bond between Thr61 and Phe63. This interaction is lost in all other peptides (Fig 3.5, Table 4.2).

Peptide Name	Peptide Sequence	Molecular Weight (g/mol)	LogP	Docking Score
P4	Ac -STEFNNTVSC- NH_2	1141.20	- 13.94	-4.893
NNA	STEFNNTVSC- NH_2	1100.17	-13.76	-5.321
NCA	Ac -STEFNNTVSC	1141.18	-16.66	-6.670
NTM	STEFNNTVSC	1100.15	-15.21	-6.625
P4'	Ac -STEFNNTVS- NH_2	1038.06	-13.45	-6.456
NNA'	STEFNNTVS- NH_2	997.03	-12.00	-7.142
NCA'	Ac -STEFNNTVS	1038.04	-16.17	-7.049
NTM'	STEFNNTVS	997.01	-14.72	-6.685

Figure 3.2 P4-Modified Peptide Physiochemical Properties and Docking Score. The peptide sequence and the end terminal modifications are shown.

A

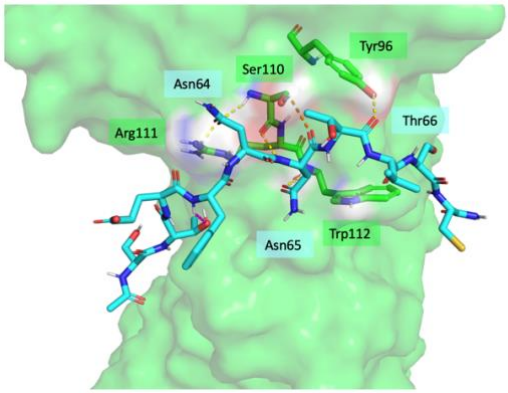

P4	Sequence: Ac-STEFNNTVSC- NH_2
	Docking Score: -4.893
	☐ Intramolecular HB between P4-Thr61 and P4-Phe63

B

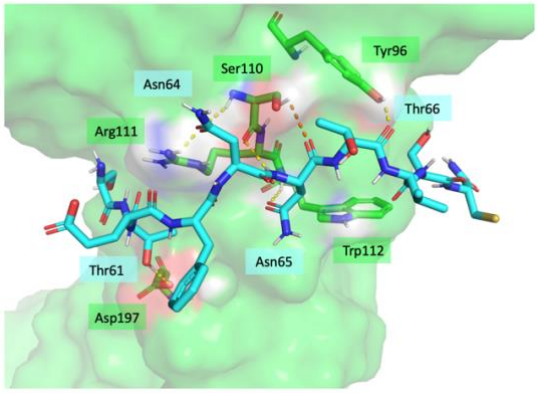

NNA	Sequence: STEFNNTVSC- NH_2
	Docking Score: -5.321
	☐ HB between NNA-Thr61 and TSLPR-Asp197

C

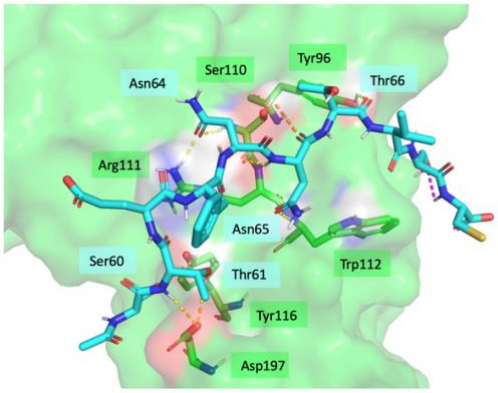

NCA	Sequence: Ac-STEFNNTVSC
	Docking Score: -6.670
	☐ Intramolecular HB between NCA-Ser68 and NCA-Cys69 ☐ HB between NCA-Ser60, NCA-Thr61 and TSLPR-Asp197 ☐ HB between NCA-Ser60 and TSLPR-Tyr116

D

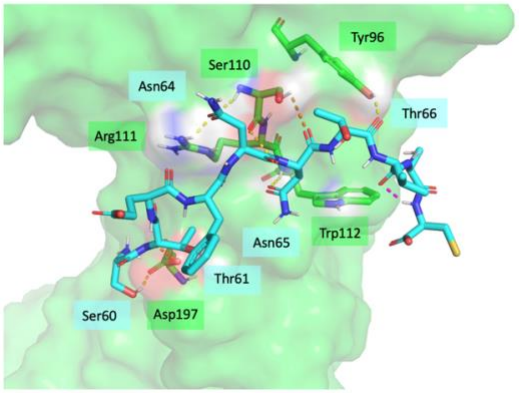

NTM	Sequence: STEFNNTVSC
	Docking Score: -6.625
	☐ Intramolecular HB between NTM-Val and NTM-Cys69 ☐ HB between NTM-Ser60, NTM-Thr61 and TSLPR-Asp197 ☐ Ionic interaction between the free N-terminal and TSLPR-Asp197

E

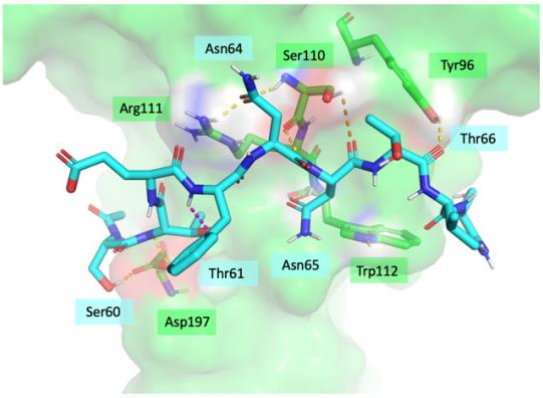

P4’	Sequence: Ac-STEFNNTVS- NH_2
	Docking Score: -6.456

- Intramolecular HB between P4’-Thr61 and P4’-Phe63
- HB between P4’-Ser60, P4’-Thr61 and TSLPR-Asp197

F

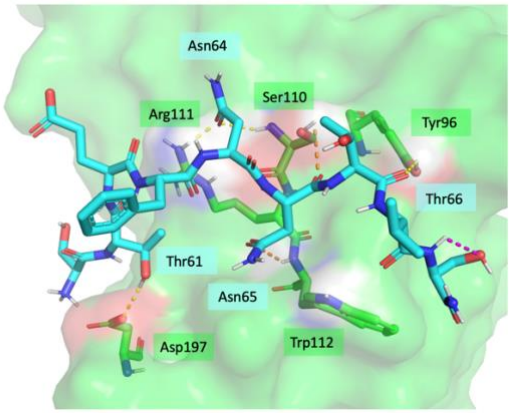

NNA’	Sequence: STEFNNTVS- NH_2
	Docking Score: -7.142

- HB within NNA’-Ser68
- HB between NNA’-Thr61 and TSLPR-Asp197
- Ionic interaction between the free N-terminal and TSLPR-Asp197

G

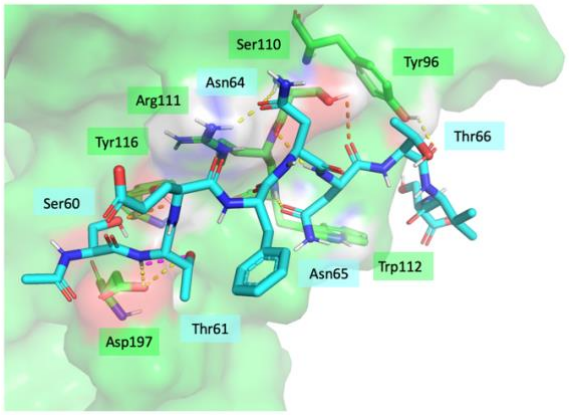

NCA’	Sequence: Ac-STEFNNTVS
	Docking Score: -7.049

- Intramolecular HB within NCA’-Thr61
- HB between NCA’-Ser60 and TSLPR-Tyr116
- HB between NCA’-Thr61’ and TSLPR-Asp197

H

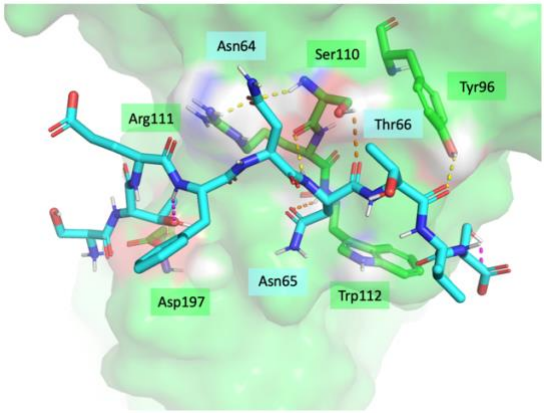

NTM’	Sequence: STEFNNTVS
	Docking Score: -6.685

- Intramolecular HB between NTM’-Thr61 and NTM’-Phe63
- Intramolecular HB between NTM’-Ser68 and the free C-terminal
- Ionic interaction between the free N-terminal and TSLPR-Asp197

Figure 3.5 Docking of the P4-Modified Peptides The surface of TSLPR is shown in translucent green. Hydrogen bonds between the fragment and the receptor are shown in yellow dashed lines. Orange dashed lines are used if the interaction was only defined by Verstraet et al. and not found using PyMol[26]. Intramolecular hydrogen bonds are shown in magenta dashed lines. For each peptide, the sequence and docking score are listed. All interactions that are made in addition to the six key interactions made by docked P4 are listed.

To confirm which of the amino acids in the P4 peptide sequence were essential for the binding of P4 to TSLPR, an alanine scan was performed using GLIDE, during which the impact on docking score of replacing each sequential amino acid with an alanine was assessed. A series of peptides numbered from 1-10 were docked with the alanine scan (P4_1, P4_2, P4_3, P4_4, P4_5, P4_6, P4_7, P4_8, P4_9, P4_10, and P4). Each number corresponds to the amino acid replaced by an alanine starting from the N-terminus. P4, P4_1, P4_6, P4_7, and P4_10 successfully docked to a similar position as the TSLP P4-fragment with the Glu62 positional constraint and the core pattern comparison, which included the backbone carbons from Phe63 to Val67 and the side chains of Phe63, Asn64, and Val67. The interactions between P4, P4_1, P4_10 and the relevant TSLPR residues are the same as six of the interactions made by the TSLP P4-fragment in the co-crystal structure (Fig 3.4). In comparison, the orientations of P4_6 and P4_7 are slightly different, even though binding involves some of the relevant residues like Arg111, Ser 110, and Tyr96.

Peptide Name	Alanine Substituted Amino Acid	Peptide Sequence	Docking Score
P4	-	Ac-STEFNNTVSC-NH_2	-6.463
P4_1	Ser	Ac-ATEFNNTVSC-NH_2	-5.824
P4_6	Asn	Ac-STEFNATVSC-NH_2	-3.172
P4_7	Thr	Ac-STEFNNAVSC-NH_2	-2.448
P4_10	Cys	Ac-STEFNNTVSA-NH_2	-5.542

Table 3.3 Docking Scores of the P4 Alanine Scan Peptides Docked to the TSLP P4-Fragment Orientation Each residue from the N terminal to the C terminal was subsequently replaced with alanine. The resulting sequences are shown alongside their docking scores.

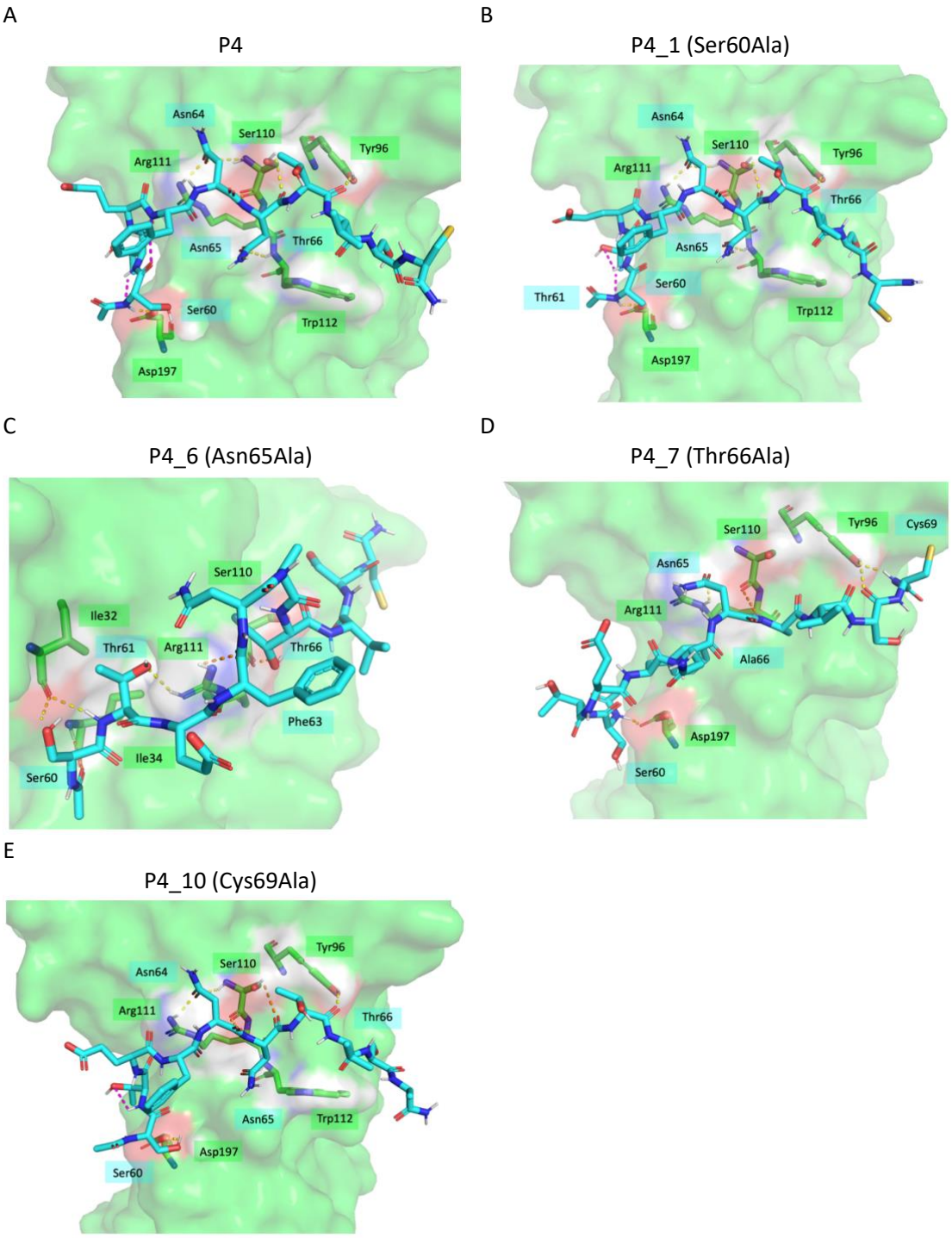

Figure 3.6 Docking of the P4 Alanine Scan Peptides to the TSLP P4-Fragment Orientation. The surface of TSLPR is shown in translucent green. Hydrogen bonds between the fragment and the receptor are shown in yellow dashed lines. Orange dashed lines are used if the interaction was only defined by the Ligand Interaction function in Maestro and not found using PyMol. Intramolecular hydrogen bonds are shown in magenta dashed lines.

The constraints used for the binding of P4_2, P4_5, P4_8, and P4_9 included at least two of the hydrogen bonding residues from the grid-based constraints. Because these constraints were not as stringent as the combination of the core pattern comparison and positional constraints used to dock P4, P4_1, P4_6, P4_7, and P4_10, the binding orientations of the remaining peptides are more variable. Finally, the docking of P4_3 only used the Glu62 positional constraint. Only one of the relevant TSLPR residues, Ser110, is involved in the interaction (Table 4.3).

Peptide Name	Alanine Substituted Amino Acid	Peptide Sequence	Docking Score
P4_2	Thr	Ac-SAEFNNTVSC-NH_2	-6.147
P4_3	Glu	Ac-STAFNNTVSC-NH_2	-4.166
P4_4	Phe	Ac-STEANNTVSC-NH_2	-1.233
P4_5	Asn	Ac-STEFANTVSC-NH_2	-9.604
P4_8	Val	Ac-STEFNNTASC-NH_2	-4.007
P4_9	Ser	Ac-STEFNNTVAC-NH_2	-2.726

Table 3.4 Docking Score of Remaining P4 Alanine Scan Peptides. Each residue from the N terminal to the C terminal was subsequently replaced with alanine. The resulting sequences are shown alongside their docking scores.

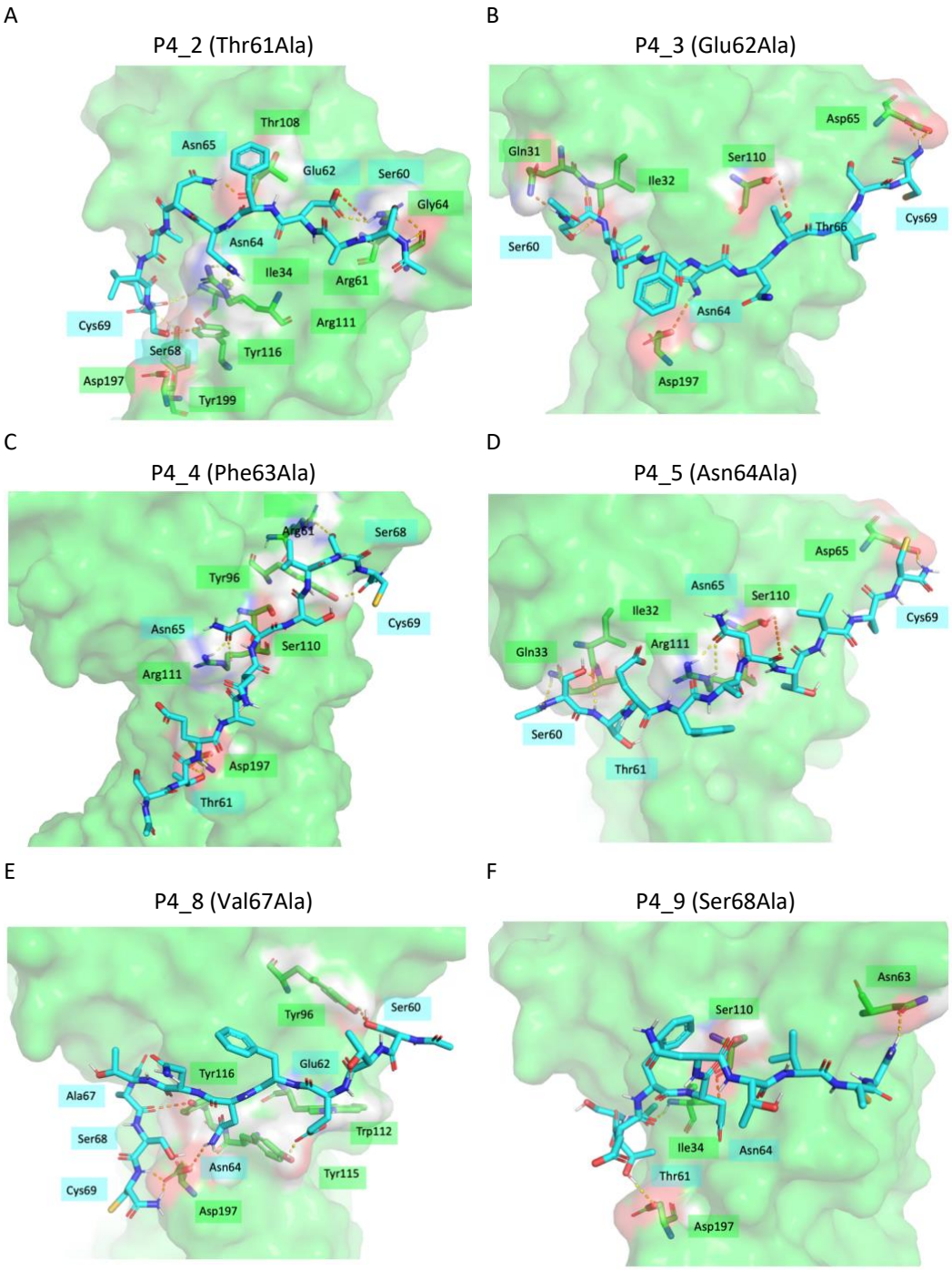

Figure 3.7 Docking of the Remaining P4 Alanine Scan Peptides. The surface of TSLPR is shown in translucent green. Hydrogen bonds between the fragment and the receptor are shown in yellow dashed lines. Orange dashed lines are used if the interaction was only defined by the Ligand Interaction function in Maestro and not found using PyMol. Intramolecular hydrogen bonds are shown in magenta dashed lines.

Based on these results, the docking scores can only be compared between P4, P4_1, P4_6, P4_7, and P4_10 as these are the only peptides with significant overlap and a binding mode congruent with the hypothesis. Removing the cysteine and the second threonine results in worse docking scores, meaning that these residues may be important for the activity of the TSLP P4-fragment. Within the context of this docking experiment, removing the residues (Asn64 and Asn65) that are predicted to be important in binding according to the interactions between the TSLP P4-fragment and TSLPR results in the loss of the hypothesized binding mode, as demonstrated by the docking of P4_5 and P4_6 (Fig 3.6, Fig 3.7).

3.4 P4-Modified Peptide Solubility

A turbidity assay was used to investigate the solubility of the P4-modified peptides and determine an appropriate solvent for future experiments. In this assay, an increase in optical density correlates to the compound reaching its solubility limit. The peptides were suspended or dissolved in either PBS or PBS + 0.5 % DMSO at concentrations that exceeded the range of the working concentrations used in future experiments. DMSO is commonly used as a co-solvent to solubilize compounds with hydrophobic characteristics, like the P4-modified peptides. At higher concentrations, DMSO can exert toxic effects on cells. Thus, the 0.5 % DMSO concentration was chosen to maximize the solubility of P4 in the solvent while minimizing cytokine inhibition and cytotoxicity. NNA demonstrated poor solubility and therefore, it was excluded from all future experiments. Most peptides showed slight insolubility at higher concentrations in PBS while this only remained true for P4 in PBS + 0.5 % DMSO. Therefore, PBS + 0.5 % DMSO was determined to be an appropriate solvent for future experiments. Although P4 exhibited slight

insolubility in PBS + 0.5 % DMSO at higher concentrations, it was included in future experiments to evaluate its effect at lower concentrations where it remained soluble in solution (Fig 2.9).

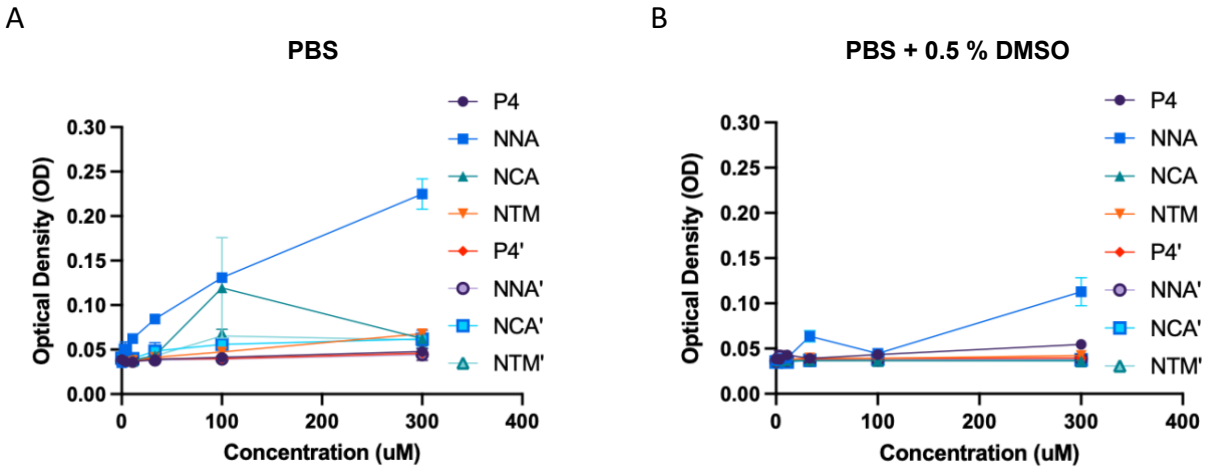

Figure 3.8 Solubility of P4-Modified Peptides. Peptides were added to either **(A)** PBS or **(B)** a PBS + 0.5 % DMSO solution at 300 µM - 11 µM (3-fold serial dilution). Optical density was measured at an absorbance of 600 nm. Error bars represent the standard error of the mean. (N = 1)

3.5 P4-Modified Peptide Screen and Assessment of Biological Activity

The P4-modified peptides were designed to target TSLPR expressed on the surface of CD4+ T cells and keratinocytes. To start testing this hypothesis, a series of ELISAs were used to screen the peptides for their biological activity in relevant cell lines and human primary cells. Firstly, the peptides were screened in HUT78 cells. These cells were activated with PMA, ionomycin, and TSLP.

P4 did not show the same level of activity when dissolved in PBS + 0.5 % DMSO (36% induction at 200 μM) compared to Milli-Q water (39 % inhibition at 200 μM). Interestingly, when compared to the vehicle control, P4 appeared to stimulate Il-13 expression instead of inhibiting it, as seen in the initial five peptides ELISA (Fig 2.4). Because P4 was not completely soluble in the initial solvent of Milli-Q water, the Il-13 results of the initial ELISA may have been an artifact of peptide precipitation (Fig 4.4). NCA, P4', and NNA' exhibited slight dose-response trends for Il-13 expression, with NCA inducing and P4' and NNA' inhibiting. No trends were observable in Il-4 expression (Fig 2.10). Importantly, the dominant effect on cytokine expression in this assay was due to the vehicle control, which had a final DMSO concentration of 0.7 % because of its role in the solvents for both the peptides and PI. The vehicle control diminished Il-13 levels by 41.9 % and Il-4 levels by 63.9 % relative to the PI + TSLP control. Because the vehicle control counteracted the effect of TSLP on Il-13 and Il-4 expression, the effect of the P4-modified peptides on TSLP signalling was not able to be determined with this screening experiment.

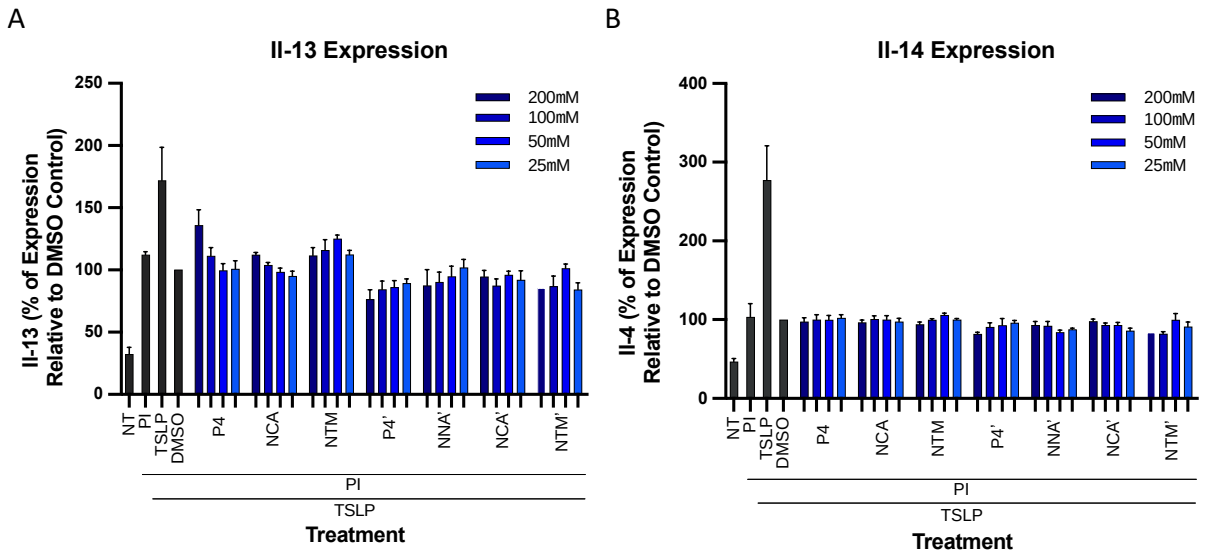

Figure 3.9 Dose Dependent Effect on Th2 Cytokine Release by the P4-Modified Peptides in HUT78 Cells. (A) shows the effect of the P4-modified peptides on Il-13 expression and **(B)** shows the effect on Il-4 expression. Error bars represent the standard error of the mean. All values are represented as percent expression relative to the DMSO control. All P4-modified peptides were tested at 200 µM – 25 µM (2-fold serial dilution). All values were compared to the DMSO control. (N = 2)

To adequately determine the effect of the P4-modified peptides on cytokine expression, it was necessary to alter the experiment. Firstly, the method of activation was switched from PI to anti-CD3/CD28 to decrease the final DMSO concentration to 0.5 %. Secondly, the cell type used was switched from HUT78 cells to primary human CD4+ T cells. Previous experimental data from the Hedtrich Laboratory suggested that the inhibitory effect of DMSO is less pronounced in CD4+ T cells than HUT78 cells. Additionally, distinct differences exist between cell lines and their primary cell counterparts, meaning that the first set of screening ELISAs performed on HUT78 cells may not accurately demonstrate the activity of the P4-modified peptides. Thus, the ELISA experiments were repeated in primary human CD4+ T cells activated with anti-CD3/CD28.

No trends were observable for the P4-modified peptides in Il-13 expression. P4, P4', NNA', and NTM' showed slight dose-responses in Il-4 inhibition (Fig 3.10). Once again, the controls in this experiment made it difficult to ascertain the effect of the P4-modified peptides on cytokine expression. DMSO decreased Il-13 levels by 23.4 % and Il-4 levels by 31.5 % compared to the CD3/CD28 + TSLP control. Although this effect was less pronounced than in HUT78 cells, the negative effect of DMSO was greater than the positive effect of TSLP on cytokine levels. Therefore, this screening experiment could not be used to elucidate the effect of the P4-modified peptides on TSLP signalling.

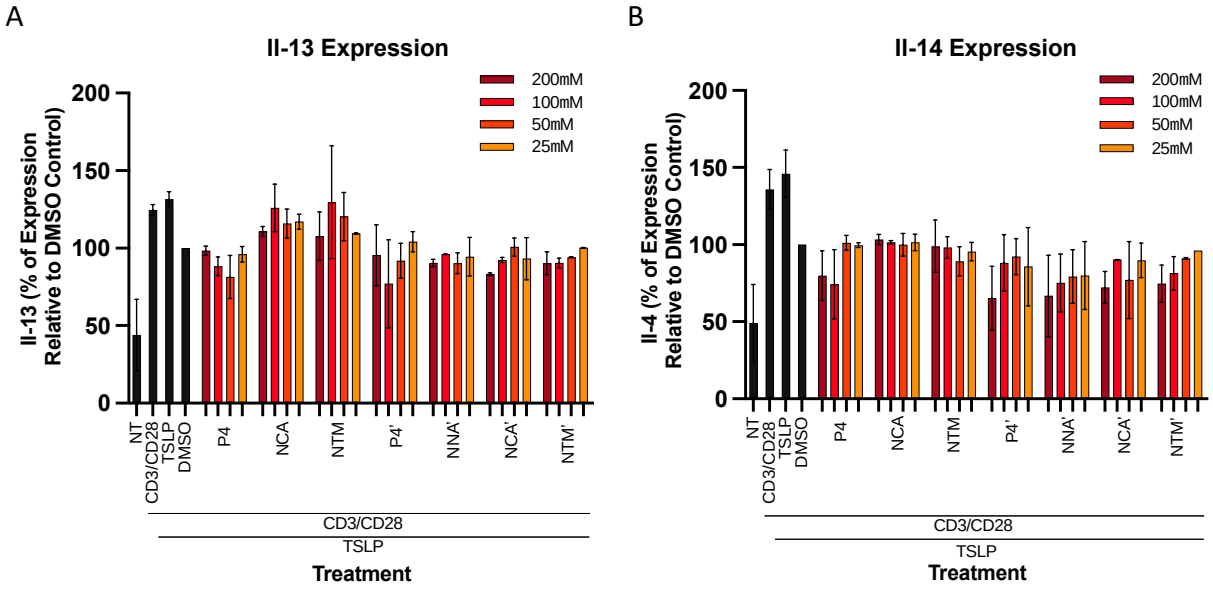

Figure 3.10 Dose Dependent Effect on Th2 Cytokine Release by the P4-Modified Peptides in CD4+ T Cells. (A) shows the effect of the P4-modified peptides on Il-13 expression and **(B)** shows the effect on Il-4 expression. Error bars represent the standard error of the mean. All values are represented as percent expression relative to the DMSO control. All P4-modified peptides were tested at 200 µM – 25 µM (2-fold serial dilution). All values were compared to the DMSO control. (N = 2)

According to these screening assays, the activity of the P4-modified peptides in both HUT78 cells and primary human CD4+ T cells was difficult to discern, likely due to combinations of low inhibitory activity, relatively small changes in cytokine expression with the addition of TSLP, and a large effect of the DMSO vehicle control. Therefore, the activity of the P4-modified peptides in keratinocytes, the second target cell type, was assessed. Keratinocytes were treated with human recombinant TSLP, with the intention that exogenous TSLP could cause the downregulation of FLG and subsequently the production of endogenous TSLP by the cells.

The human TSLP ELISA kit utilized recognizes both endogenously produced and recombinant human TSLP, meaning that the cytokine reading may include the recombinant TSLP used to stimulate the keratinocytes as well as the TSLP produced by the keratinocytes. The concentration of TSLP detected by the ELISA ranged from 425 – 14 138 pg/mL. These levels are lower than the treatment concentration of extrinsic TSLP, which may be due to degradation of the extrinsic TSLP. This would be expected given the 36 h incubation time, yet the effects of TSLP signal activation would be expected to persist at this time point.

Unlike the previous two screening ELISAs in HUT78 cells and primary human CD4+ T cells, the vehicle control, which contained 0.5 % DMSO, did not have a significant effect on cytokine expression compared to the human recombinant TSLP control. Furthermore, the addition of recombinant human TSLP increased TSLP expression by 1193.2 % compared to the non-treated control. Interestingly, P4, NCA, NTM and NCA' showed a large dose-dependent effect on TSLP expression. 200 µM and 100 µM of P4, 200 µM of NCA, 200 µM and 100 µM of NTM, and 200 µM and 100 µM NCA' showed statistically significant reduction of TSLP levels (Fig 3.11). This

assay suggests that P4, NCA, NTM, and NCA' may inhibit TSLP signalling in primary keratinocytes.

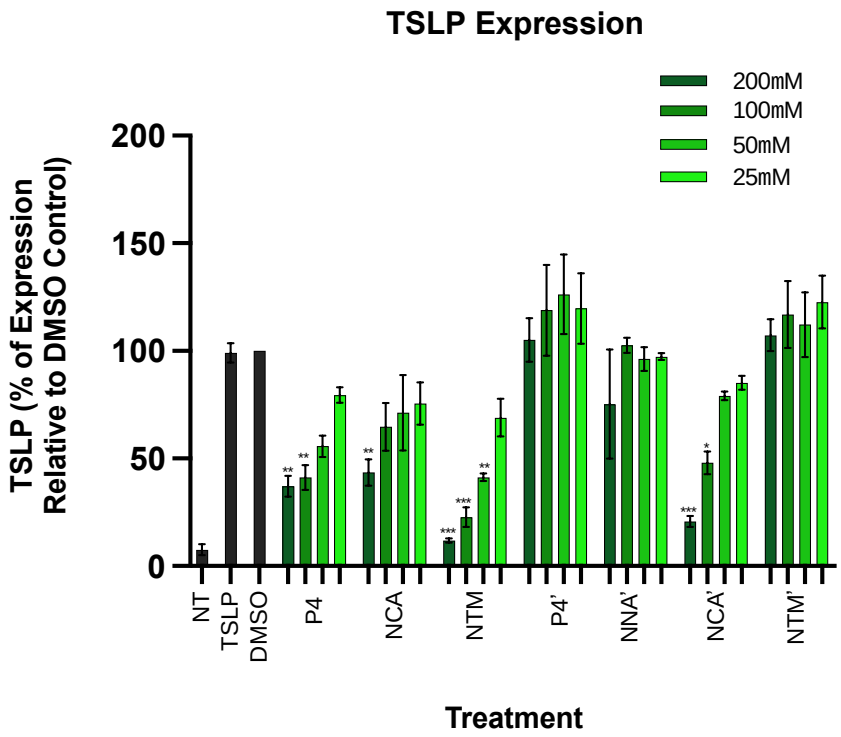

Figure 3.11 Dose Dependent Inhibition of TSLP Release by the P4-Modified Peptides in Keratinocytes. Error bars represent the standard error of the mean. All values are represented as percent expression relative to the DMSO control. All P4-modified peptides were tested at 200 µM – 25 µM (2-fold serial dilution). All values were compared to the DMSO control. *p < 0.05, **p < 0.01, ***p < 0.001, ns not indicated. (N = 3)

3.6 P4-Modified Peptide Biocompatibility

The skin is comprised of three main layers: the epidermis, which is composed primarily of keratinocytes, the dermis, in which fibroblasts are the primary cell type, and the hypodermis. Because the P4-modified peptides are intended to be a topically applied therapeutic, they will encounter keratinocytes in the epidermis. Although the peptides are not expected to be skin

permeable, reformulation and permeability enhancers may allow them to reach fibroblasts in the dermis. Furthermore, the compromised epidermal integrity present in AD may allow infiltration of traditionally non-permeable compounds into deeper layers of the skin. Therefore, the biocompatibility of the peptides with both keratinocytes and fibroblasts was tested using an MTT assay. Decreased signal in the MTT assay may result from at least three related phenomena: (1) Inhibition of metabolic activity, which could be caused by impaired mitochondria function, (2) Decreased cell proliferation; as cells were assayed under exponential growth conditions, compounds that slow cell replication would reduce cell numbers compared to controls, resulting in lower signal. (3) Cytotoxic effects; compounds that kill the cells would reduce cell numbers and therefore decrease signal.

In keratinocytes, the highest concentrations of all the P4-modified peptides except P4 showed statistically significant differences in metabolic activity compared to the DMSO control. This was not the case for subsequently lower concentrations of NCA, NTM, and NNA'. High concentrations of P4 may have not impacted cell viability because of insolubility, as aggregation of the peptide may hinder any effect of the peptide on the cell. Compared to keratinocytes, the compounds showed less of an effect in fibroblasts. 200 μM of P4' as well as 200 μM and 100 μM of NCA' showed statistically significant impairment of metabolic activity (Fig 3.12). None of the compounds reduced the signal to a similar level to the no cells control, indicating that they may not be overtly toxic, and may more likely induce a growth arrest or affect metabolic processes at these high concentrations.

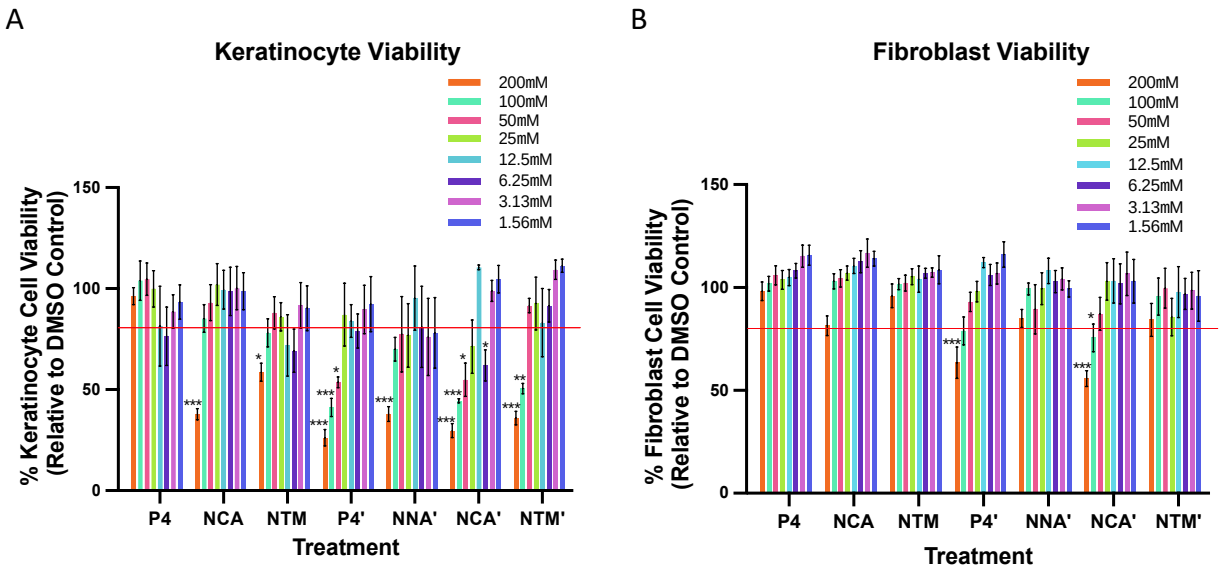

Figure 3.12 Effect of P4-Modified Peptides on Cell Viability Assessed Using the MTT Assay. **(A)** Primary human keratinocytes and **(B)** fibroblasts were treated with the P4-modified peptides at the concentrations 200 µM - 1.562 µM (2-fold serial dilution). Error bars represent the standard error of the mean. All values are represented as percent expression relative to the DMSO control. All values were compared to the DMSO control. *p < 0.05, **p < 0.01, ***p < 0.001, ns not indicated. (N = 4)

Because the MTT assay measures metabolic activity, it can not be used as a stand-alone method to determine cytotoxicity, as treatment may result in lower metabolic activity while the cells remain alive. To help determine the nature of the effects observed in the MTT assay, the Live and Dead Cell Stain assay was used, which assesses membrane permeability which is compromised upon cell death. The TSLP ELISAs showed that the peptides with the highest potencies showed activity at both 200 µM and 100 µM. Therefore, 100 µM was chosen as the treatment concentration for the Live and Dead Cell Assay.

The fluorescent images were semi-quantified using an ImageJ macro which adjusted the image so each cell or nucleus was identified as a particle, resulting in the number of live and dead cells respectively. This method was used for all peptides except NTM in fibroblasts. Because the

fluorescent red masses in these images could not be appropriately quantified using the same method as the other treatments, each dead cell was manually counted. Semi-quantification of the fluorescent images obtained from the Live and Dead Cell assay shows that P4' treatment results in statistically significant cell death in keratinocytes. The effect of P4' on keratinocytes was predicted by the MTT assay. All other peptides do not demonstrate cytotoxicity relative to the DMSO control (Fig 3.13).

A

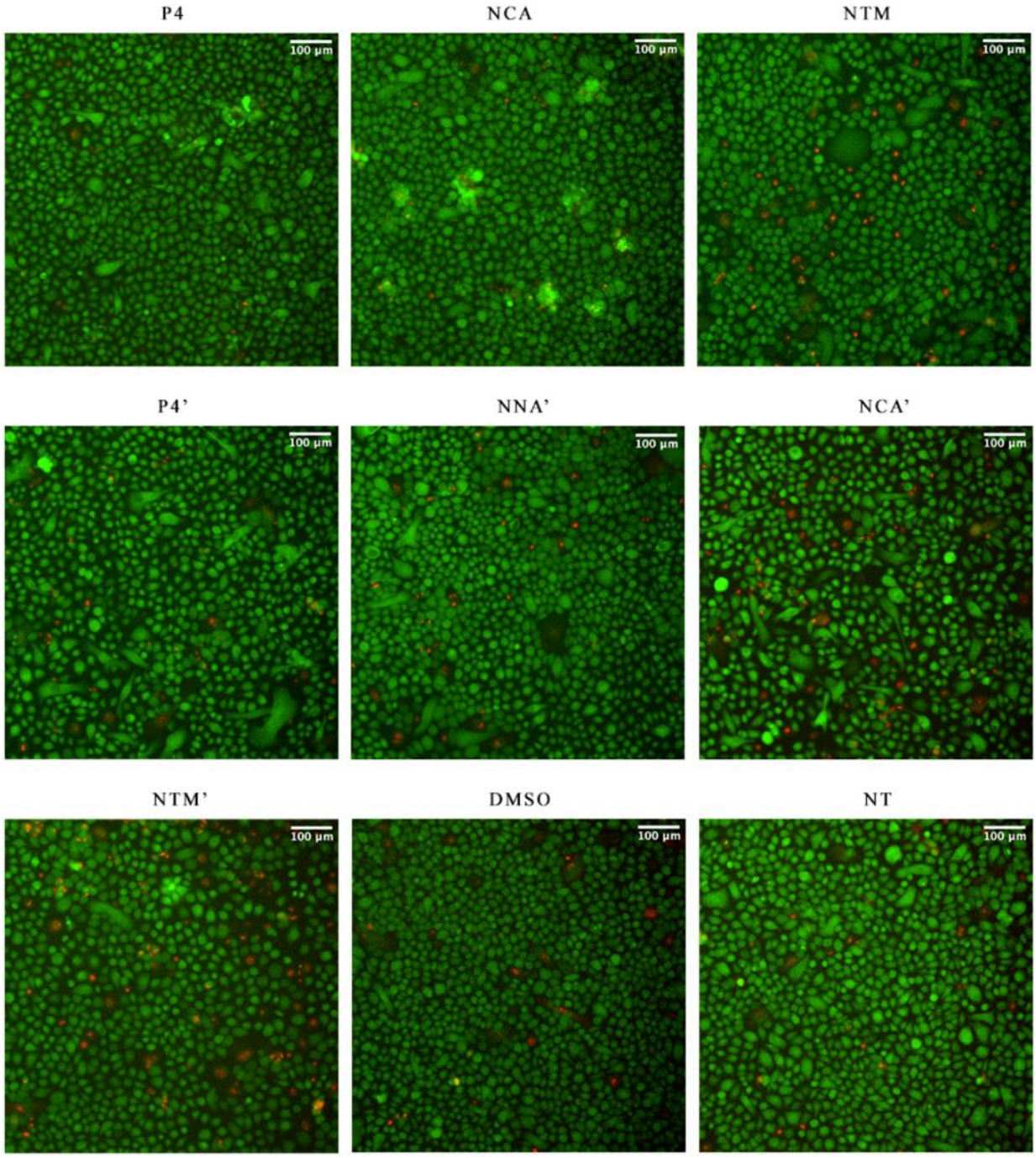

B

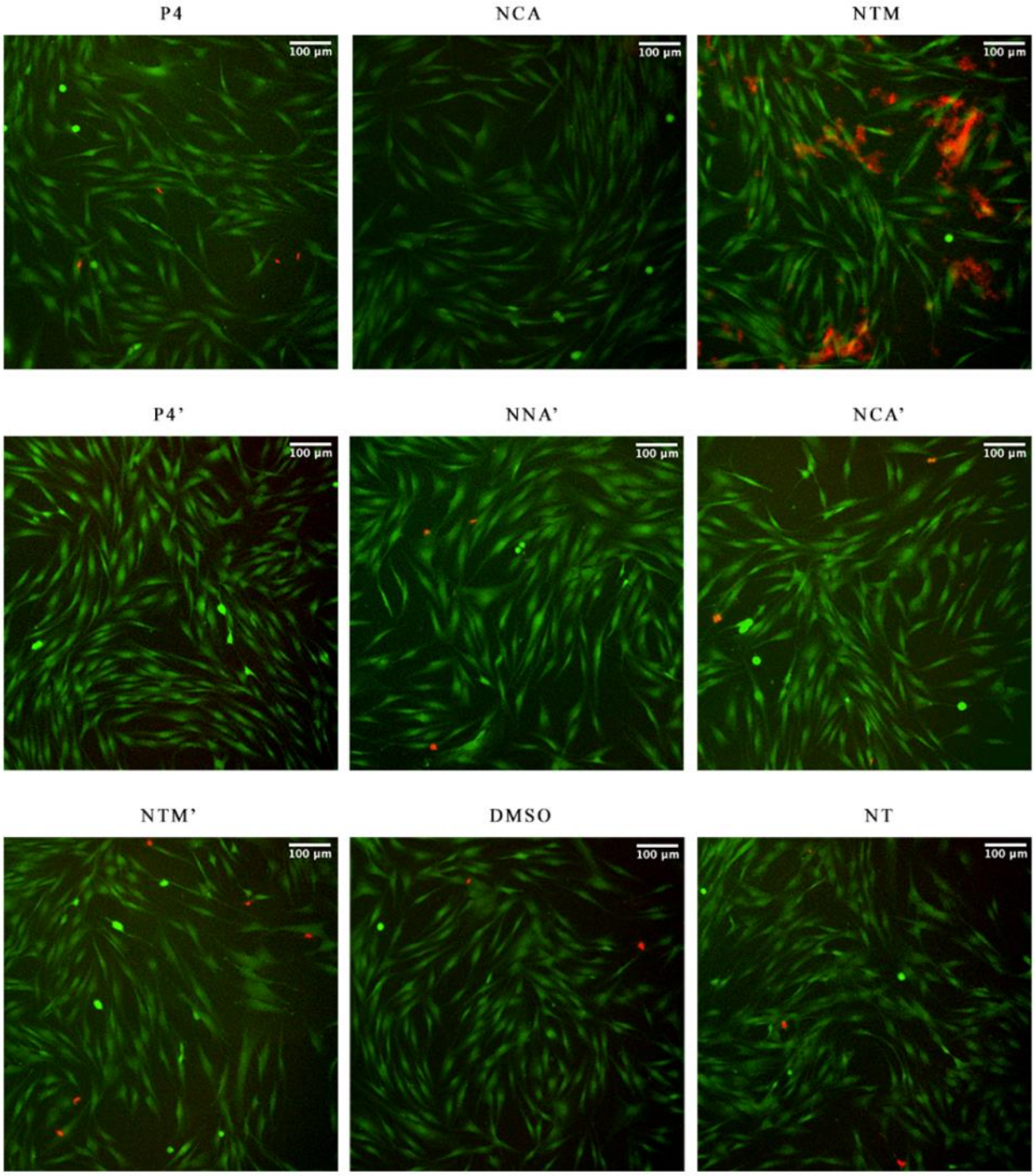

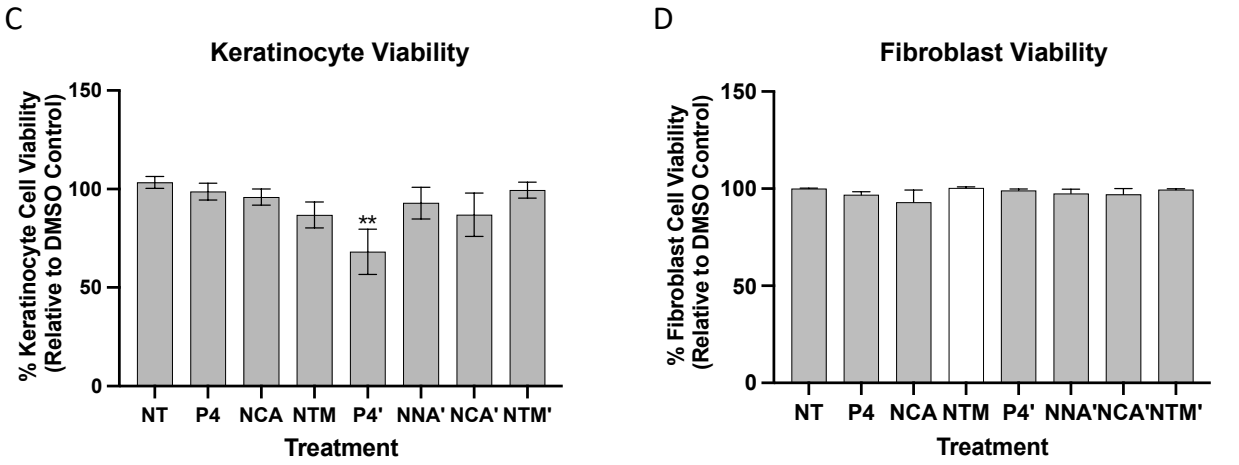

Figure 3.13 Effect of P4-Modified Peptides on Cell Viability Assessed Using the Live and Dead Cell Stain Assay. (A) Keratinocytes and **(B)** fibroblasts were treated with 100 µM of each P4-modified peptide and the cells were imaged using fluorescence microscopy. The images were semi-quantified using ImageJ. Semi-quantified **(C)** keratinocyte and **(D)** fibroblast data are presented. The NTM-treated fibroblast data is shown as a patterned bar as opposed to solid gray because the dead cells were manually counted instead of quantified using a macro. Error bars represent the standard error of the mean. All values are represented as percent expression relative to the DMSO control. All values were compared to the DMSO control *p < 0.05, **p < 0.01, ***p < 0.001, ns not indicated. (N = 3)

3.7 Discussion

Although there has been progress in developing small molecule drugs and therapeutic antibodies for the treatment of AD, the use of peptides and peptidomimetics remain to be fully explored within this space. Recently, Liu *et al.* reported the use of a broad-spectrum anti-inflammatory topical peptide called the Nuclear Import Checkpoint Inhibitor for the treatment of a mouse AD model[81]. It targets two nuclear transport shuttles to inhibit the expression of TSLP, Il-4, Il-4Rα, Il-1β, Il-6, Il-13, Il-23α, Il-33, IFN-γ, GM-CSF, VEGF A, RANTES, Il-8, COX-2 and iNOS. Many of these are cytokines that are involved in the pathophysiology of AD while others like iNOS have more diverse functions. In addition, antimicrobial peptides have been considered for the treatment of AD because of the role of dysbiosis of the skin microbiome. Parnassin is a

tetrapeptide that is predicated to have anti-microbial properties[82]. When applied topically on AD mouse models, it was shown to improve skin lesions. Although both reported peptides show efficacy in AD mouse models, their mechanism of action is not specific to the pathophysiology of AD. Park *et al.* developed a set of 16 peptides based on two sequences of murine TSLPR and evaluated them for their ability to bind to murine TSLP[83]. Using an ELISA, they determined that these peptides inhibited the interaction between TSLP and TSLPR at 1 mM - 0.1 mM. They were able to determine that including a tryptophan at the C terminus of the original sequence increased potency. Inhibition of the interaction between TSLP and TSLPR by these probes suggests that TSLP may be a druggable target. Similarly, here we describe the use of peptides designed based on the interaction sites of the TSLPR-TSLP-IL7Rα complex as pharmacological probes to investigate the druggability of TSLPR. Unlike Park *et al*, these peptides were based on TSLP and IL7Rα sequences that may interact with TSLPR[84]. The resulting lead compounds can be used as the foundation for the development of potent peptide-based AD therapeutics.

The peptides developed in this project were screened for their activity in HUT78 cells and in CD4+ T cells. In these assays, the vehicle control demonstrated a complete reversal of cytokine expression induced by TSLP in HUT78 cells and this was exacerbated in the CD4+ T cell ELISA. Due to the poor controls, these assays could not adequately determine the effect of the peptides on TSLP signalling through the detection of Il-13 and Il-4 levels.

Although it is difficult to compare the compounds because of the poor controls in the screening assays, trends for cell type differences and differential cytokine expression can be observed. The P4-modified peptides affect both the T cell ELISAs differently based on the cell type tested

(HUT78 or CD4+ T cell) and the cytokine detected (Il-13 or Il-4). Although HUT78 cells are considered to be analogous to activated CD4+ T cells, the ELISAs show clear cell type dependent differences in the activity of the P4-modified peptides (Fig 3.9, Fig 3.10). The protocol for each experiment slightly differs, with HUT78 cells being activated by PI while CD4+ T cells were activated with anti-CD3/CD28. Although the hypothesized mechanism of action of the P4-modified peptides is independent of the initial activation method, they may exert an effect on these pathways, leading to the differences between the HUT78 and CD4+ T cell ELISA results. Alternatively, activation with these methods may alter TSLPR expression in different ways. Currently, there is minimal literature comparing TSLPR expression changes on T cells as a response to PI and anti-CD3/CD28 activation. In addition to cell type specific differences in the ELISA results, Il-13 and Il-4 expression patterns do not always mirror each other. These differences may be because of the slight differential regulation of Il-13 and Il-4 expression[85]. Both cytokines are secreted by CD4+ T cells that have been polarized to Th2 cells and their corresponding genes are located in the same vicinity on chromosome 5, in an area called the Th2 cytokine locus. Although they share many regulatory elements and share a receptor subunit, the mechanisms by which they are produced are slightly different, with Il-4 production being calcineurin-dependent while the same is only partially true for Il-13[85]. Calcineurin is a component of a pathway that regulates the expression of many cytokine genes in Th2 cells. Guo *et al.* found that inhibiting calcineurin partially blocked the production of Il-13 and fully blocked the production of Il-4 in murine CD4+ T cells activated by PI[86]. This means that Il-4 production completely relies on the calcium-calcineurin-NFAT pathway while Il-13 production is only partially dependent on calcineurin and also involves the NF-κB pathway[87].

The P4-modified peptides may interact with these pathways to differentially affect Il-13 and Il-4 production.

In comparison to the HUT78 and CD4+ T cell screening ELISAs, the keratinocyte ELISA had appropriate controls, where the vehicle control did not completely diminish the effect of adding recombinant human TSLP on cytokine expression. Therefore, the effect of the P4-modified peptides on TSLP signalling was able to be investigated through the keratinocyte ELISA, showing P4, NCA, NTM, and NTM' as having inhibitory effects.

The hypothesized mechanism of action of the initial five peptides and the P4-modified peptides is that they interact with TSLPR or IL7Rα in the same way as their corresponding fragment in the TSLP-TSLPR-IL7Rα complex. The docking experiments were not completely predictive of the biological activity assessment by the TSLP ELISA. P4, which was predicted to have the worst binding affinity, showed statistically significant activity in the TSLP ELISA. However, NTM showed the highest activity in the TSLP ELISA and had a good docking score relative to P4. The predicted interactions included two additional hydrogen bonds and ionic interactions between NTM and TSLPR-Asp197. This extensive interaction with TSLPR-Asp197 may translate to increased biological activity. A similar combination of interactions was predicted in NTM', which also demonstrated significant biological activity. However, NNA' broke this pattern by showing no activity in the TSLP ELISA despite being predicted to have the best binding affinity for TSLPR. Both NCA and NCA' were predicated to interact with TSLPR-Tyr116, had relatively good docking scores, and exhibited significant biological activity. Overall, the complexity of cell-based assays may account for the discrepancy between the

docking results and the TSLP ELISA. Factors such as peptide stability and promiscuity may result in the lack of translation of docking scores to biological activity.

After evaluating the biological activity, the P4-modified peptides were assessed for biocompatibility using the MTT assay and the Live and Dead Cell Stain assay. The MTT assay uses metabolic activity while the Live and Dead Cell Stain uses membrane permeability as an indicator of cytotoxicity. The MTT assay assesses metabolic activity by assessing the ability of cells to transform the MTT reagent to formazan crystals through the NADPH dependent oxidoreductase enzymes present in the mitochondria[88]. It is difficult to differentiate between a reduction in cellular metabolism as a result of cytotoxicity or drug-induced metabolic suppression[89]. To be a viable measure for cell viability, MTT assay results must be considered alongside another method of assessing toxicity, like the Live and Dead Cell Stain assay, which uses membrane permeability as a measure of cytotoxicity. The decrease in metabolic activity after treatment with some peptides did not completely translate to a decrease in membrane permeability. P4' is the only peptide that is confirmed to be cytotoxic as it shows significant effects in both cytotoxicity assays in keratinocytes. Although keratinocyte metabolic activity was impaired after treatment with 100 μM NNA', NCA' and NTM', these peptides did not have statistically significant effects on membrane permeability. Although fibroblast metabolic activity was impaired after treatment with 100 μM NCA', it did not have a statistically significant effect on membrane permeability.

P4' did not demonstrate the same level of cytotoxicity in the Live Dead Cell Assay as it did in the MTT assay in fibroblasts. A confounding factor that limits the comparison between these two

assays is the confluency of the fibroblasts. To limit the signal-to-noise ratio, there needed to be enough cell free area in the images. Otherwise, a haze of green fluorescence was observed in the images, making them difficult to semi-quantify. Therefore, the Live Dead Cell Assay in fibroblasts was performed at a lower confluency than the MTT assays. This may have altered the mechanism by which P4' affected the cells. For example, cell death can occur at a higher rate in very confluent cell cultures[90]. If the health of the P4' treated cells in the MTT assay was already compromised due to high confluency, the cytotoxic effects of the treatment may be more evident. This change in confluency was not necessary for the keratinocyte Live Dead Cell Assay as the signal-to-noise ratio in the fluorescence images at a high confluency did not impede the semi-quantification of the data.

In the Live and Dead Cell Stain assay, the NTM treated fibroblasts initially show statistically significant cytotoxicity after semi-quantification using the macro developed. This was because the red dye stained large masses of material instead of distinct points within the cell that would correspond to the DNA in the nuclei. The MTT assay did not show a decrease in metabolic activity that would be expected if treatment with NTM was causing cells to die and release their nuclear material. Therefore, it is likely that these red masses do not correspond to DNA. It is possible that the dye used to identify dead cells is interacting with the treatment peptide instead. The reason that this is only seen in the fibroblasts may be because of differences in cell culture conditions such as the media used. Therefore, NTM' treated fibroblasts were subsequently semi-quantified manually instead of using the macro (Fig 3.13D).

The cytotoxicity data can be considered alongside the TSLP ELISA to investigate the mechanism by which peptide treatment results in a decrease in TSLP levels. Both the hypothesized mechanism of action and a decrease in cell viability can result in the decrease in TSLP expression seen in the TSLP ELISA. NCA' is the only peptide that both decreased metabolic activity in keratinocytes and significantly reduced TSLP levels. Although the cytotoxicity was not corroborated by the Live and Dead Cell Stain Assay, the minimal activity and the large decrease in metabolic activity is enough reason to eliminate NCA' as a lead compound. However, a decrease in metabolic activity does not necessarily correspond to a decrease in biological activity. Like NCA', P4' also shows significant cytotoxicity in the MTT assays at higher concentrations yet does not result in a decrease in TSLP expression. This leaves P4, NCA, and NTM as potential lead compounds for further study.

CHAPTER 4: Evaluation of Small Molecule Inhibitors of TSLP Signalling

Previously, the Hedtrich and Page Laboratories jointly developed small molecule inhibitors of TSLPR through virtual screening, docking, and iterative chemical synthesis. After virtually screening a library of compounds and testing 12 select compounds that were predicted to interact with the TSLPR-TSLP-IL7Rα complex using a HUT78 ELISA, C7 and C13 emerged as leads (Sup 3). A series of analogues were produced based on the structure of C7 and C13, which led to the development of BP79, a potent inhibitor of Il-13 and Il-4 expression as determined by a HUT78 ELISA (Fig 4.1). Additional inactive compounds were also identified, including BP75 which was used as a negative control for future experiments. This novel small molecule was further characterized through CD4+ T cell ELISAs, western blots detecting downstream signalling components of the TSLP signalling pathway like pSTAT3 and pSTAT5, a proximity ligation assay, and thermal shift assays. This previous work demonstrates that BP79 efficiently binds to and inhibits TSLP-dependent signalling. Further characterization of BP79 was necessary, including assessing its biocompatibility with relevant cell types and ability to penetrate the skin.

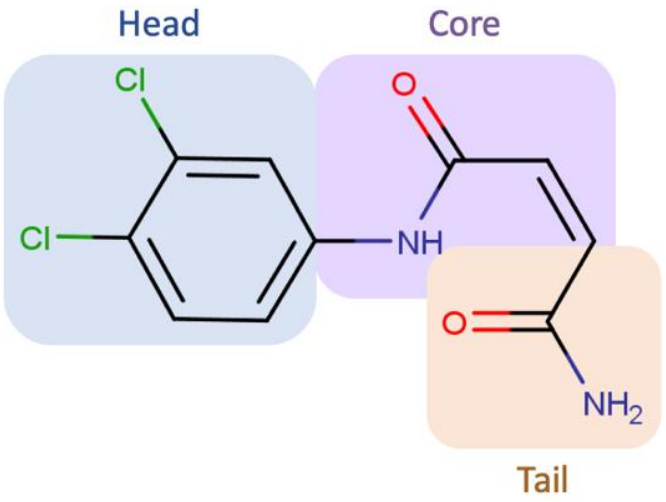

Figure 3.1 Chemical Structure of BP79. The substituted phenyl head is shown in blue, the amide and alkene core is shown in purple, and the terminal amide is shown in orange.

4.1 BP79 Biocompatibility

An MTT assay was used to evaluate the cytotoxicity of BP79 and BP75 by assessing their effect on metabolic activity. Because BP79 is intended to be a topically applied therapeutic, its biocompatibility with keratinocytes was assessed. As a small molecule, the molecular weight of BP79 falls below the 500 Da threshold necessary for skin penetration. Additionally, BP79 had a logP value of 1.74, which falls between the necessary range (logP = 1 - 3) for skin penetration. Because of its favourable logP, it was assumed that BP79 may passively permeate through the skin, causing it to encounter fibroblasts in the dermis. Therefore, the cytotoxicity of BP79 on fibroblasts was assessed as well. Additionally, skin barrier defects present in AD may facilitate penetration of topical therapeutics to deeper skin layers, including the dermis.

The cell viability of BP79 and BP75 was tested at 20 μM - 0.156 μM (2-fold dilutions). This is firstly because the BP79 ELISA demonstrated statistically significant inhibition of Il-13 and Il-4

production at all concentrations tested (20 μM - 5 μM (2-fold serial dilution)). Secondly, the C7 and C13 ELISAs demonstrated statistically significant inhibition of Il-13 production at all concentrations tested (20 μM - 0.25 μM (2-fold serial dilution)). The efficacy at the lowest concentration of C7 and C13 did not seem to plateau, suggesting that it could be effective at even lower concentrations. Based on C13 and C7, BP79 may also be active at 0.25 μM or even lower. None of the concentrations tested demonstrated a statistically significant effect on cell viability in this assay (Fig 4.2). A biologically significant threshold for the MTT assay is 80 % cell viability relative to the DMSO control. None of the tested compounds fell below this threshold except 20 μM of BP79 in keratinocytes (Fig 4.2 A).

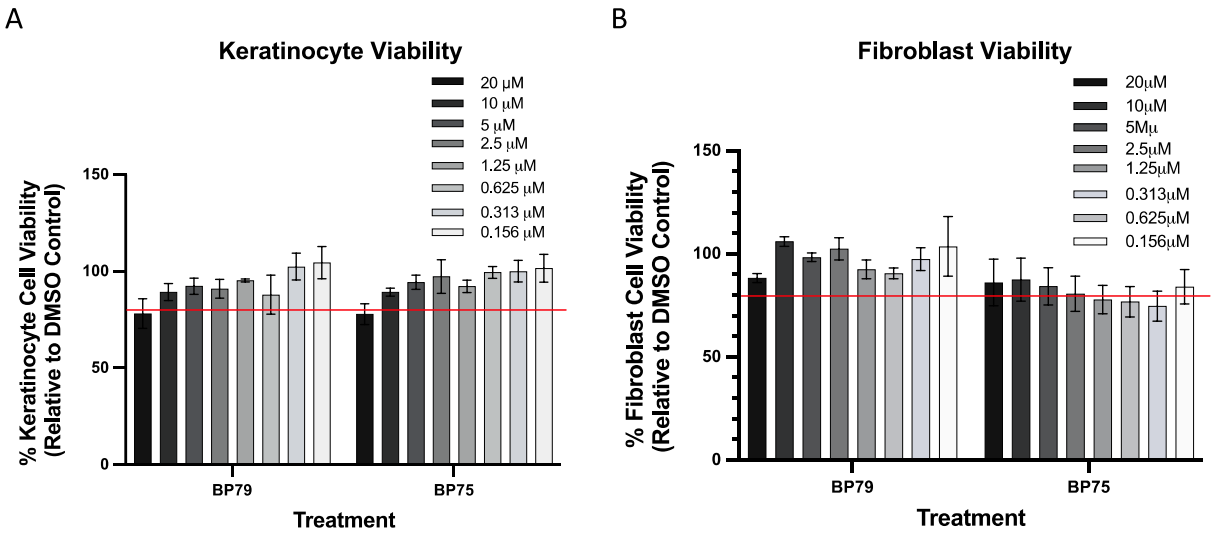

Figure 4.2 Effect of BP79 and BP75 on Cell Viability Assessed Using the MTT Assay. (A) Keratinocytes (N = 4) and **(B)** fibroblasts (N = 5) were treated with the small molecules at concentrations ranging from 20 μM - 1.56 μM (2-fold serial dilutions). Error bars represent the standard error of the mean. All values are represented as percent expression relative to the DMSO control. All values were compared to the DMSO control. *p < 0.05, **p < 0.01, ***p < 0.001, ns not indicated.

4.2 BP79 Skin Absorption

A skin absorption test was performed to determine the extent to which BP79 penetrates through human skin. BP79 was allowed to penetrate excised human skin mounted onto diffusion Franz cells for 24, 8, 4, and 2 h. The amount of BP79 that had passed through the skin and entered the PBS in the Franz cell body was determined by measuring its concentration via LC/MS by the Chemistry Analytical department (UBC, Pharmaceutical Sciences) (Sup 4). Skin absorption was detected at 8 h (~150 nM) and enhanced at 24 h (~380 nM). However, this effect cannot be solely attributed to the desirable physiochemical properties of BP79, as the vehicle chosen was 100 % DMSO. DMSO is known to enhance skin penetration by disrupting the barrier function of the stratum corneum. Additionally, DMSO is cytotoxic at high concentrations, which may further contribute to the penetration of the BP79 formulation used in this assay. Reformulation of the BP79 solution in the future should use alternative safe and effective concentrations of other chemical skin penetration enhancers.

4.3 Small Molecule Screen and Assessment of Biological Activity

BP79 is composed of a substituted phenyl ring, an amide core, and an alkene attached to a terminal amide (Fig 4.1). A series of small molecules were designed based on the structure of BP79 by the Page Laboratory through the incorporation of various chemical moieties to the terminal amide of BP79 (Sup 5). These compounds were made with the intention of establishing a structure-activity relationship and developing a more potent lead compound. The biological activity of these BP79 analogues was investigated in HUT78 cells using an ELISA. The first set of compounds was screened at three concentrations (20 μM – 5 μM (2-fold serial dilution)) and

exhibited potencies similar to BP79. The HUT78 ELISAs use a final DMSO concentration of 0.4 %, as it was the solvent for both the novel compounds as well as PI, which were responsible for 0.2 % each. The vehicle control brings Il-4 levels from the PI+TSLP control almost down to the PI control, making it difficult to differentiate between cytokine inhibition by DMSO and by the compounds themselves (Fig 4.3).

To more clearly delineate the potencies of the compounds, the protocol was altered by testing all compounds at 1 μM. Once again, DMSO almost completely reversed the cytokine expression induced by TSLP, making it difficult to delineate between the DMSO effect and the effect of the small molecule inhibitors. Despite the DMSO effect, the assay showed that 12 compounds decreased Il-13 expression. Additionally, 8 compounds retained the activity of BP79, meaning that the structural modifications made to these were tolerated (Fig 4.3 C, D).

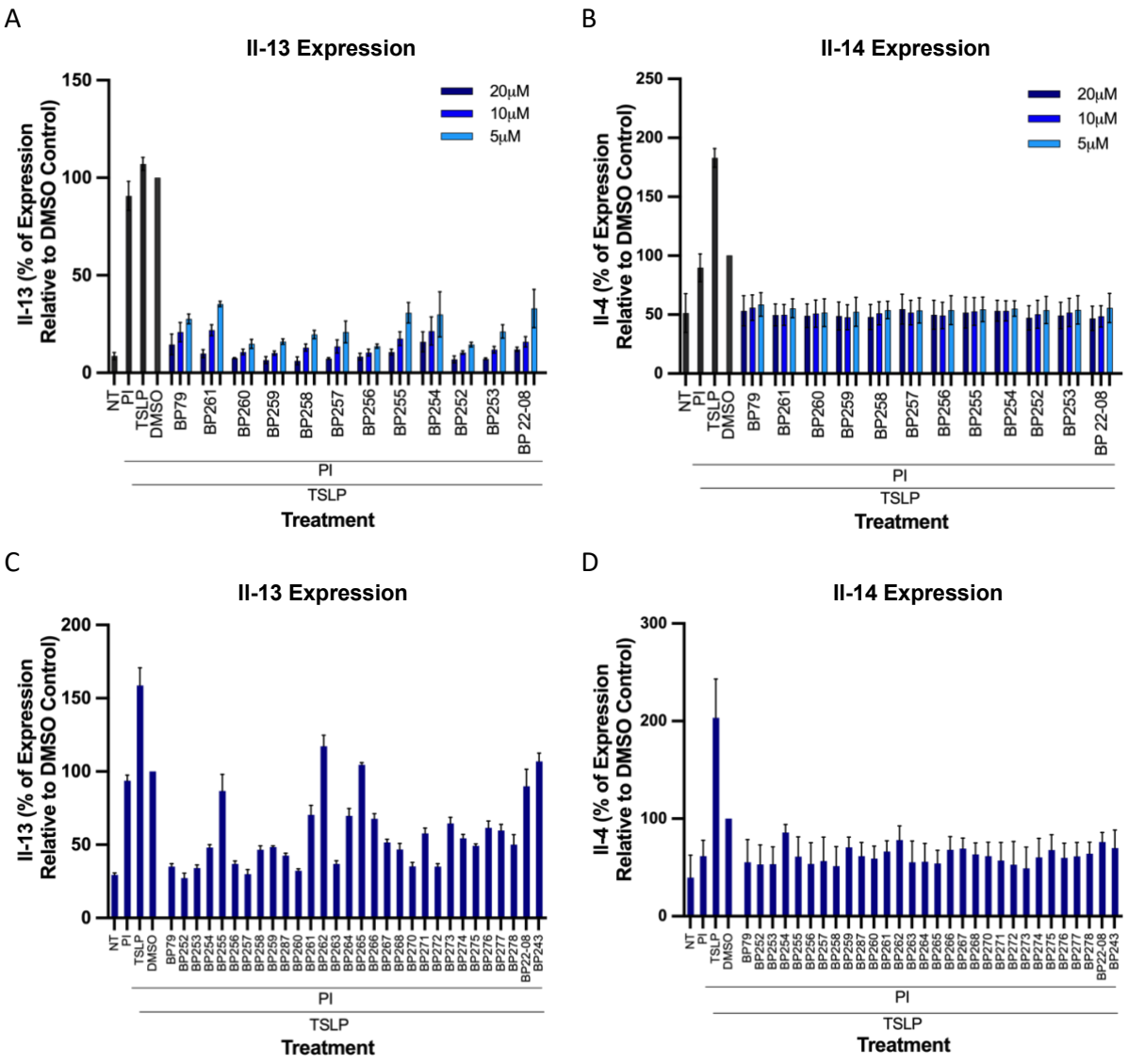

Figure 4.3 Inhibition of Th2 Cytokine Release by the BP79 Analogues in HUT78 Cells. All compounds were first tested at 20 µM – 5 µM (2-fold serial dilution) and the effect on **(A)** Il-13 levels and **(B)** Il-4 levels were assessed. Subsequently, the compounds were tested at 1µM and the effect on **(C)** Il-13 levels and **(D)** Il-4 levels were assessed. Error bars represent the standard error of the mean. All values are represented as percent expression relative to the DMSO control. All values were compared to the DMSO control. (N = 2)

To further investigate the BP79 analogues that retained their activity in an assay that more closely mimics human AD, they were tested in primary human CD4+ T cells using an ELISA. In addition to being more physiologically relevant, this assay was performed with the intention of

mitigating the large vehicle effect on cytokine release seen in the previous HUT78 ELISAs. The effect of the vehicle was further minimized by altering the concentration of DMSO in the treatment, for a final concentration of 0.01 % DMSO. Of the 28 new compounds tested, 8 had similar potencies to BP79 at 1 μM (Fig 4.3 C, D). From these 8, 7 had structurally diverse modifications and were chosen for assessment in CD4+ T cells. BP265 which showed minimal Il-13 inhibition at 1 μM, was chosen as a negative control. This compound replaced BP75 as the negative control because it was more structurally similar to BP79 while still being inactive. These compounds were tested at the concentrations 1000 nM – 111 nM (3-fold serial dilution) (Fig 4.4).

The alterations made to the ELISA protocol to prevent the inhibitory effect of DMSO on cytokine release were successful. However, the addition of TSLP did not significantly increase cytokine expression relative to the CD3/CD28 control. The inhibition of cytokine release by the compounds was compared to the respective BP79 concentrations. 111 nM of BP252, 333 nM and 111 nM of BP256, all concentrations of BP263, and 333 nM of BP270 showed statistically significant differences in Il-13 expression when compared to BP79. However, none of these compounds showed higher potencies than BP79 at any concentration, and are therefore not indicated in the graph as statistically significant. Il-4 expression did not show any statistically significant differences compared to BP79 (Fig 4.4). All other compounds were equipotent compared to BP79.

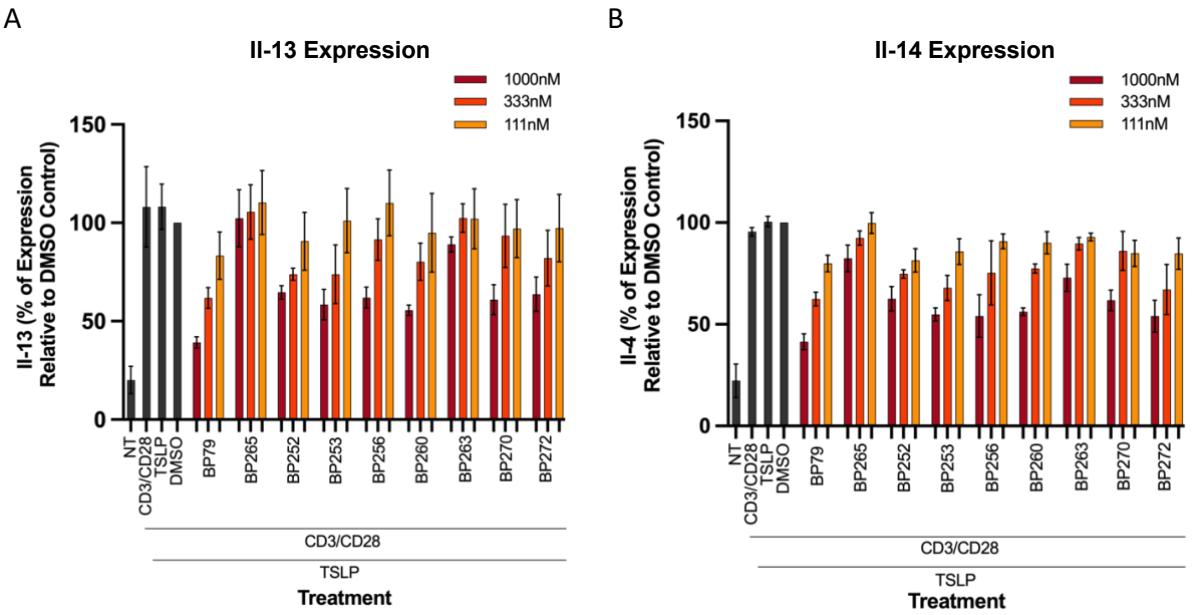

Figure 4.4 Inhibition of Th2 Cytokine Release by the Most Potent BP79 Analogues in CD4+ T Cells. All compounds were tested at 1000 nM - 111.1 nM and the effect on **(A)** Il-13 levels and **(B)** Il-4 levels were assessed. Error bars represent the standard error of the mean. All values are represented as percent expression relative to the DMSO control. All values were compared to their corresponding BP79 concentration, which was the positive control. *p < 0.05, **p < 0.01, ***p < 0.001, ns not indicated. (N = 3)

4.4 Discussion

AD is a heterogeneous disease, as it can involve many types of immune responses (Th2, Th1, and Th17) and has a complex etiology[91]. Therefore, there are many molecular targets for novel AD therapeutics. The recent small molecules that have been developed to treat AD include JAK inhibitors[92]. Although these were developed to be systemic drugs through oral administration, they can be reformulated as topical treatments[57]. However, developing JAK inhibitors without pleiotropic effects is difficult because these kinases are key components in many signalling pathways[93]. Topical JAK inhibitors include ruxolitinib, which has FDA approval, and delgocitinib, which has been approved in Japan for the treatment of AD[94, 95]. Many of these inhibitors have been associated with mild to moderate local adverse effects including itching and

acne as well as systemic effects like nasopharyngitis[96]. Nakagawa *et al.* performed a long-term safety and efficacy study of topical delgocitinib and found that 15.4 % of patients experienced treatment-related adverse effects, the most prevalent of which was nasopharyngitis[97]. The occurrence of systemic immunosuppressive effects as a result of a topical JAK inhibitor suggests that they may exert broader than intended biological effects. However, the FDA warning labels do not differentiate between on-target and off-target induced adverse effects, making it difficult to conclude that the side effects of topical JAK inhibitors are from on-target interactions that act beyond the intended system. In comparison to JAKs, TSLPR is responsible primarily for the Th2 immune response, which is characteristic of AD. Although the TSLP signalling pathway involves JAK1/2, targeting TSLPR does not prevent JAK1/2 from functioning in other pathways. Thus, targeting the TSLPR signalling pathway may provide more specificity for the treatment of AD in comparison to topical JAK inhibitors. BP79 is a small molecule that was developed and extensively characterized by the Hedtrich and Page Laboratories and has the potential to become a topically administered treatment for AD and the prevention of the atopic march.

A series of modifications were made to BP79 with the intention of improving potency and determining a structure-activity relationship. These compounds were then evaluated for their activity in T cells using both HUT78 cells and primary human CD4+ T cells using an ELISA. One of the primary issues in this set of assays was the effect of the vehicle control on cytokine levels detected. A large DMSO effect made it difficult to delineate between the potency of the compounds themselves and the effect of the vehicle. There are many possible mechanisms by which DMSO exerts its effects on cytokine levels. Holthaus *et al.* showed that the cytokines released by CD4+ T cells were affected at 0.25 % and 1 % DMSO, with Il-4 levels dropping to

84.2 % and 70.5 % of untreated levels respectively[98]. This effect may contribute to the drastic decrease in cytokine release seen in the HUT78 ELISAs. Another explanation is that proliferation of CD4+ T cells is affected by DMSO. Proliferation and activation of these cells have been shown to decrease at a DMSO concentration of 0.25 % and be progressively reduced up to 1 %. Specifically, proliferation was shown to stagnate after treatment with 1 % DMSO. Although the ELISAs used to screen the small molecules did not have concentrations as high as 1 %, the DMSO concentration used for the HUT78 ELISAs may still have an effect on proliferation and activation. However, these effects were not expected to be seen with final DMSO concentrations of 0.01 %. Therefore, the ELISAs performed in CD4+ T cells were more representative of the potencies of the compounds tested.

CHAPTER 5. Conclusion and Future Directions

The TSLP signalling cascade is a master regulator of the type 2 immune response characteristic of AD, making it an attractive pathway to target with inhibitory therapeutics[25]. Many types of inhibitors have been investigated for treating the symptoms and the cause of AD, including biologics, small molecules, and peptides to a lesser extent[84, 94, 96]. Systemic therapies like biologics and some oral JAK inhibitors are usually reserved for moderate to severe forms of AD. Oral JAK inhibitors like tofacitinib and upadacitinib are effective but also have black box warnings for heart attack and stroke, and thus should only be used where safer treatments fail. Therapeutics like topical JAK inhibitors are more tolerable and have the potential for pleiotropic effects[93]. Meanwhile, topical peptide inhibitors of TSLPR are in the very early stages of the drug development pipeline and currently are only being used as molecular probes[84]. Due to the lack of consistently effective topical therapies that target specific components of the pathophysiology of AD, there remains the need for further therapeutic development.

Peptide and small molecule-based approaches were employed to explore the druggability of TSLPR. Using the peptide approach, it is difficult to say for certain that TSLPR is a druggable target. Of the P4-modified peptides, P4, NCA, and NTM were the most promising according to the keratinocyte ELISA and the cell viability assays. However, further characterization is needed to confirm that these peptides are interacting with TSLPR in a similar manner to the endogenous sequences they were based on. Using the small molecule approach more conclusively established TSLPR as a druggable target. This is because BP79 had previously undergone extensive characterization that demonstrated a potent interaction with TSLPR, which was able to alter

TSLP signalling. The BP79 analogues that were evaluated for biological activity demonstrated that modifications made to the original structure resulted in a change in potency in the T cell ELISAs. Although none were more potent, they all still affected the TSLP signalling pathway, further establishing the druggability of TSLPR.

Both the lead peptides and lead small molecule will need to undergo further characterization and optimization to make them more drug-like. For the lead peptides, it is necessary to establish that they interact with TSLPR. For example, thermal stability assays can evaluate the ability of the lead compound to stabilize the TSLPR while exposed to a range of temperatures[100]. The proximity ligation assay is a cellular assay in which fluorescence is used to determine if Il7Rα and TSLPR engage with each other in the presence of the compounds[101]. TSLPR and Il7Rα antibodies can be used to visualize the co-localization of the co-receptors and how addition of the lead peptides affects this in the presence of TSLP. If the lead peptides interact with any component of the ternary complex to prevent the interaction between TSLP and its heterodimeric receptor, fluorescence signal will be lost. To further establish that the lead peptides inhibit the TSLP signalling pathway, their effect on more upstream components should be assessed. In keratinocytes, a western blot detecting FLG could be used to determine if the compounds inhibit TSLP signalling, causing a downregulation in FLG, and a subsequent downregulation in TSLP production. Another signalling component in this pathway is pSTAT3, which can also be detected using a western blot. Further iterative design and evaluation will be necessary to eventually develop a peptidomimetic based on the initial lead peptides identified here. This optimization will include chemical modifications that increase potency and stability, likely resulting in more small molecule-like features.

The lead small molecule is also in the early stages of drug development. Although it has already been extensively characterized through previous work done in the Page and Hedtrich Laboratories, it will need to undergo further selectivity and pharmacokinetic analysis. Because BP79 is predicted to penetrate the skin and possibly enter circulation based on the logP values and the skin absorption assay, the hepatic metabolism of the compound should be investigated. This can be done with a microsomal stability assay in which liver microsomes with cytochrome P450 enzymes are incubated with the lead compound and the NADPH co-factor[102]. The resulting supernatant will be analyzed using LC/MS for the presence of the initial lead compound.

Therapeutics based on the lead peptides and small molecule may not only treat AD but also prevent the atopic march. As the first atopic disease in the progression of the atopic march, AD is an attractive target[4]. Epidemiologic studies have found that AD, food allergy, allergic rhinitis, and allergic asthma are often comorbid. Although the exact mechanism that connects these atopic diseases has not been elucidated, the TSLP signalling pathway can be involved in the pathogenesis of all four conditions[103]. As topical therapeutics that target the TSLP signalling pathway, drugs based on the lead peptides and small molecules may prevent the progression of the atopic march. This effect can be evaluated using the microfluidic organ-on-chip model developed by the Hedtrich Laboratory. This model links the skin, bronchial epithelial models, and lymph node-like structures using activated CD4+ T cells in the circulating media to emulate the immune response associated with AD.

Although there are many AD therapeutics, there are few that are effective in all severities, can be topically applied, and target specific components of the pathophysiology of AD to minimize pleiotropic effects. The TSLP signalling pathway has been characterized as a key component of AD and thus is a promising target for novel topical inhibitors. Peptide and small molecule inhibitors of TSLPR were developed and evaluated to further establish the druggability of TSLPR. Overall, the work presented here has contributed to advancing the understanding of TSLP signalling and its potential inhibition. This may contribute to the development of better treatment options for AD and help alleviate the debilitating symptoms faced by patients.

REFERENCES

1. Nutten, S. Atopic Dermatitis: Global Epidemiology and Risk Factors. *Ann. Nutr. Metab.* **66**, 8–16 (2015).
2. Beattie, P. E. & Lewis-Jones, M. S. A comparative study of impairment of quality of life in children with skin disease and children with other chronic childhood diseases. *Br. J. Dermatol.* **155**, 145–151 (2006).
3. Barbeau, M. & Bpharm, H. L. Burden of Atopic dermatitis in Canada. *Int. J. Dermatol.* **45**, 31–36 (2006).
4. Bantz, S. K., Zhu, Z. & Zheng, T. The Atopic March: Progression from Atopic Dermatitis to Allergic Rhinitis and Asthma. *J. Clin. Cell. Immunol.* **5**, 202 (2014).
5. Elias, P. M. & Steinhoff, M. "Outside-to-Inside" (and Now Back to "Outside") Pathogenic Mechanisms in Atopic Dermatitis. *J. Invest. Dermatol.* **128**, 1067–1070 (2008).
6. Losquadro, W. D. Anatomy of the Skin and the Pathogenesis of Nonmelanoma Skin Cancer. *Facial Plast. Surg. Clin. N. Am.* **25**, 283–289 (2017).
7. Rice, G. & Rompolas, P. Advances in resolving the heterogeneity and dynamics of keratinocyte differentiation. *Curr. Opin. Cell Biol.* **67**, 92–98 (2020).
8. Deo, P. N. & Deshmukh, R. Pathophysiology of keratinization. *J. Oral Maxillofac. Pathol. JOMFP* **22**, 86–91 (2018).
9. Sandilands, A., Sutherland, C., Irvine, A. D. & McLean, W. H. I. Filaggrin in the frontline: role in skin barrier function and disease. *J. Cell Sci.* **122**, 1285–1294 (2009).
10. Moosbrugger-Martinz, V. *et al.* Revisiting the Roles of Filaggrin in Atopic Dermatitis. *Int. J. Mol. Sci.* **23**, 5318 (2022).

11. Nedoszytko, B. *et al.* Genetic and Epigenetic Aspects of Atopic Dermatitis. *Int. J. Mol. Sci.* **21**, 6484 (2020).
12. Cvitas, I., Galichet, A., Ling, S. C., Müller, E. J. & Marti, E. Toll-like receptor-ligand induced thymic stromal lymphopoietin expression in primary equine keratinocytes. *Vet. Dermatol.* **31**, 154 (2020).
13. Sroka-Tomaszewska, J. & Trzeciak, M. Molecular Mechanisms of Atopic Dermatitis Pathogenesis. *Int. J. Mol. Sci.* **22**, 4130 (2021).
14. Reddy, A. & Fried, B. Chapter 3 Atopic Disorders and Parasitic Infections. in *Advances in Parasitology* vol. 66 149–191 (Academic Press, 2008).
15. Brandt, E. B. & Sivaprasad, U. Th2 Cytokines and Atopic Dermatitis. *J. Clin. Cell. Immunol.* **2**, 110 (2011).
16. Cote-Sierra, J. *et al.* Interleukin 2 plays a central role in Th2 differentiation. *Proc. Natl. Acad. Sci. U. S. A.* **101**, 3880–3885 (2004).
17. Napolitano, M., di Vico, F., Ruggiero, A., Fabbrocini, G. & Patruno, C. The hidden sentinel of the skin: An overview on the role of interleukin-13 in atopic dermatitis. *Front. Med.* **10**, 1165098 (2023).
18. Jovanovic, K., Siebeck, M. & Gropp, R. The route to pathologies in chronic inflammatory diseases characterized by T helper type 2 immune cells. *Clin. Exp. Immunol.* **178**, 201–211 (2014).
19. Mitamura, Y. *et al.* The IL-13/periostin/IL-24 pathway causes epidermal barrier dysfunction in allergic skin inflammation. *Allergy* **73**, 1881–1891 (2018).
20. Furue, K. *et al.* The IL-13–OVOL1–FLG axis in atopic dermatitis. *Immunology* **158**, 281–286 (2019).

21. Mishra, S. K. *et al.* Periostin Activation of Integrin Receptors on Sensory Neurons Induces Allergic Itch. *Cell Rep.* **31**, 107472 (2020).

22. Furue, M. Regulation of Filaggrin, Loricrin, and Involucrin by IL-4, IL-13, IL-17A, IL-22, AHR, and NRF2: Pathogenic Implications in Atopic Dermatitis. *Int. J. Mol. Sci.* **21**, 5382 (2020).

23. Junttila, I. S. Tuning the Cytokine Responses: An Update on Interleukin (IL)-4 and IL-13 Receptor Complexes. *Front. Immunol.* **9**, 888 (2018).

24. Wollenberg, A., Thomsen, S. F., Lacour, J.-P., Jaumont, X. & Lazarewicz, S. Targeting immunoglobulin E in atopic dermatitis: A review of the existing evidence. *World Allergy Organ. J.* **14**, 100519 (2021).

25. Adhikary, P. P., Tan, Z., Page, B. D. G. & Hedtrich, S. TSLP as druggable target – a silver-lining for atopic diseases? *Pharmacol. Ther.* **217**, 107648 (2021).

26. Verstraete, K. *et al.* Structure and antagonism of the receptor complex mediated by human TSLP in allergy and asthma. *Nat. Commun.* **8**, 14937 (2017).

27. Zhong, J. *et al.* TSLP signaling pathway map: a platform for analysis of TSLP-mediated signaling. *Database J. Biol. Databases Curation* **2014**, bau007 (2014).

28. Varricchi, G. *et al.* Thymic Stromal Lymphopoietin Isoforms, Inflammatory Disorders, and Cancer. *Front. Immunol.* **9**, 1595 (2018).

29. Yang, G. *et al.* Skin Barrier Abnormalities and Immune Dysfunction in Atopic Dermatitis. *Int. J. Mol. Sci.* **21**, 2867 (2020).

30. Luo, J. *et al.* The Role of TSLP in Atopic Dermatitis: From Pathogenetic Molecule to Therapeutical Target. *Mediators Inflamm.* **2023**, 7697699 (2023).

31. Zhang, K. *et al.* Constitutive and inducible thymic stromal lymphopoietin expression in human airway smooth muscle cells: role in chronic obstructive pulmonary disease. *Am. J. Physiol. Lung Cell. Mol. Physiol.* **293**, L375-382 (2007).
32. Kato, A., Favoreto, S., Avila, P. C. & Schleimer, R. P. TLR3- and Th2 Cytokine-Dependent Production of Thymic Stromal Lymphopoietin in Human Airway Epithelial Cells. *J. Immunol. Baltim. Md 1950* **179**, 1080–1087 (2007).
33. Čepelak, I., Dodig, S. & Pavić, I. Filaggrin and atopic march. *Biochem. Medica* **29**, 020501 (2019).
34. Lee, K. H. *et al.* Filaggrin knockdown and Toll-like receptor 3 (TLR3) stimulation enhanced the production of thymic stromal lymphopoietin (TSLP) from epidermal layers. *Exp. Dermatol.* **20**, 149–151 (2011).
35. Moniaga, C. S. *et al.* Protease Activity Enhances Production of Thymic Stromal Lymphopoietin and Basophil Accumulation in Flaky Tail Mice. *Am. J. Pathol.* **182**, 841–851 (2013).
36. Cianferoni, A. & Spergel, J. The importance of TSLP in allergic disease and its role as a potential therapeutic target. *Expert Rev. Clin. Immunol.* **10**, 1463–1474 (2014).
37. Dai, X. *et al.* TSLP Impairs Epidermal Barrier Integrity by Stimulating the Formation of Nuclear IL-33/Phosphorylated STAT3 Complex in Human Keratinocytes. *J. Invest. Dermatol.* **142**, 2100-2108.e5 (2022).
38. Soumelis, V. *et al.* Human epithelial cells trigger dendritic cell mediated allergic inflammation by producing TSLP. *Nat. Immunol.* **3**, 673–680 (2002).
39. Rochman, Y. *et al.* TSLP signaling in CD4+ T cells programs a pathogenic T helper 2 cell state. *Sci. Signal.* **11**, eaam8858 (2018).

40. Keegan, A. D., Leonard, W. J. & Zhu, J. Recent advances in understanding the role of IL-4 signaling. *Fac. Rev.* **10**, 71 (2021).

41. Locksley, R. M. Asthma and allergic inflammation. *Cell* **140**, 777–783 (2010).

42. Yang, L., Fu, J. & Zhou, Y. Research Progress in Atopic March. *Front. Immunol.* **11**, 1907 (2020).

43. T, H. *et al.* Association study of childhood food allergy with genome-wide association studies-discovered loci of atopic dermatitis and eosinophilic esophagitis. *J. Allergy Clin. Immunol.* **140**, (2017).

44. Mohammad, A. A. *et al.* Prevalence of atopic comorbidities in eosinophilic esophagitis: A case-control study of 449 patients. *J. Am. Acad. Dermatol.* **76**, 559–560 (2017).

45. Belgrave, D. C. M., Simpson, A., Buchan, I. E. & Custovic, A. Atopic Dermatitis and Respiratory Allergy: What is the Link. *Curr. Dermatol. Rep.* **4**, 221 (2015).

46. Zhang, Z. *et al.* Thymic stromal lymphopoietin overproduced by keratinocytes in mouse skin aggravates experimental asthma. *Proc. Natl. Acad. Sci. U. S. A.* **106**, 1536–1541 (2009).

47. Noti, M. *et al.* Exposure to food allergens through inflamed skin promotes intestinal food allergy through the thymic stromal lymphopoietin-basophil axis. *J. Allergy Clin. Immunol.* **133**, 1390–1399, 1399.e1–6 (2014).

48. Frazier, W. & Bhardwaj, N. Atopic Dermatitis: Diagnosis and Treatment. *Am. Fam. Physician* **101**, 590–598 (2020).

49. Johnson, B. B., Franco, A. I., Beck, L. A. & Prezzano, J. C. Treatment-resistant atopic dermatitis: challenges and solutions. *Clin. Cosmet. Investig. Dermatol.* **12**, 181–192 (2019).

50. Gabros, S., Nessel, T. A. & Zito, P. M. Topical Corticosteroids. in *StatPearls* (StatPearls Publishing, 2023).

51. Drucker, A. M. *et al.* Use of systemic corticosteroids for atopic dermatitis: International Eczema Council consensus statement. *Br. J. Dermatol.* **178**, 768–775 (2018).
52. Ferrucci, S. M., Tavecchio, S., Marzano, A. V. & Buffon, S. Emerging Systemic Treatments for Atopic Dermatitis. *Dermatol. Ther.* **13**, 1071–1081 (2023).
53. Padda, I. S., Bhatt, R. & Parmar, M. Upadacitinib. in *StatPearls* (StatPearls Publishing, 2023).
54. Ahmad, A., Zaheer, M. & Balis, F. J. Baricitinib. in *StatPearls* (StatPearls Publishing, 2023).
55. Padda, I. S., Bhatt, R. & Parmar, M. Tofacitinib. in *StatPearls* (StatPearls Publishing, 2023).
56. Samuel, C., Cornman, H., Kambala, A. & Kwatra, S. G. A Review on the Safety of Using JAK Inhibitors in Dermatology: Clinical and Laboratory Monitoring. *Dermatol. Ther.* **13**, 729–749 (2023).
57. Bissonnette, R. *et al.* Topical tofacitinib for atopic dermatitis: a phase IIa randomized trial. *Br. J. Dermatol.* **175**, 902–911 (2016).
58. Harb, H. & Chatila, T. Mechanisms of Dupilumab. *Clin. Exp. Allergy J. Br. Soc. Allergy Clin. Immunol.* **50**, 5–14 (2020).
59. Silverberg, J. I. *et al.* Two Phase 3 Trials of Lebrikizumab for Moderate-to-Severe Atopic Dermatitis. *N. Engl. J. Med.* **388**, 1080–1091 (2023).
60. Renert-Yuval, Y. & Guttman-Yassky, E. New treatments for atopic dermatitis targeting beyond IL-4/IL-13 cytokines. *Ann. Allergy. Asthma. Immunol.* **124**, 28–35 (2020).
61. Puar, N., Chovatiya, R. & Paller, A. S. New treatments in atopic dermatitis. *Ann. Allergy. Asthma. Immunol.* **126**, 21–31 (2021).

62. Menzies-Gow, A. *et al.* Long-term safety and efficacy of tezepelumab in people with severe, uncontrolled asthma (DESTINATION): a randomised, placebo-controlled extension study. *Lancet Respir. Med.* **11**, 425–438 (2023).

63. Menzies-Gow, A. *et al.* DESTINATION: a phase 3, multicentre, randomized, double-blind, placebo-controlled, parallel-group trial to evaluate the long-term safety and tolerability of tezepelumab in adults and adolescents with severe, uncontrolled asthma. *Respir. Res.* **21**, 279 (2020).

64. Wang, X., Ni, D., Liu, Y. & Lu, S. Rational Design of Peptide-Based Inhibitors Disrupting Protein-Protein Interactions. *Front. Chem.* **9**, (2021).

65. Vinogradov, A. A., Yin, Y. & Suga, H. Macrocyclic Peptides as Drug Candidates: Recent Progress and Remaining Challenges. *J. Am. Chem. Soc.* **141**, 4167–4181 (2019).

66. Walensky, L. D. & Bird, G. H. Hydrocarbon-Stapled Peptides: Principles, Practice, and Progress. *J. Med. Chem.* **57**, 6275–6288 (2014).

67. Wang, L. *et al.* Therapeutic peptides: current applications and future directions. *Signal Transduct. Target. Ther.* **7**, 1–27 (2022).

68. Katsila, T., Siskos, A. P. & Tamvakopoulos, C. Peptide and protein drugs: The study of their metabolism and catabolism by mass spectrometry. *Mass Spectrom. Rev.* **31**, 110–133 (2012).

69. Craik, D. J., Fairlie, D. P., Liras, S. & Price, D. The Future of Peptide-based Drugs. *Chem. Biol. Drug Des.* **81**, 136–147 (2013).

70. Singh, N., Kalluri, H., Herwadkar, A., Badkar, A. & Banga, A. K. Transcending the skin barrier to deliver peptides and proteins using active technologies. *Crit. Rev. Ther. Drug Carrier Syst.* **29**, 265–298 (2012).

71. Trabocchi, A. Chapter 6 - Principles and applications of small molecule peptidomimetics. in *Small Molecule Drug Discovery* (eds. Trabocchi, A. & Lenci, E.) 163–195 (Elsevier, 2020). doi:10.1016/B978-0-12-818349-6.00006-6.

72. Tsomaia, N. Peptide therapeutics: Targeting the undruggable space. *Eur. J. Med. Chem.* **94**, 459–470 (2015).

73. Ali, A. M., Atmaj, J., Van Oosterwijk, N., Groves, M. R. & Dömling, A. Stapled Peptides Inhibitors: A New Window for Target Drug Discovery. *Comput. Struct. Biotechnol. J.* **17**, 263–281 (2019).

74. Di, L. Strategic Approaches to Optimizing Peptide ADME Properties. *AAPS J.* **17**, 134–143 (2014).

75. Fosgerau, K. & Hoffmann, T. Peptide therapeutics: current status and future directions. *Drug Discov. Today* **20**, 122–128 (2015).

76. Román, J., Castillo, A. & Mahn, A. Molecular Docking of Potential Inhibitors of Broccoli Myrosinase. *Mol. J. Synth. Chem. Nat. Prod. Chem.* **23**, 1313 (2018).

77. Anthis, N. J. & Clore, G. M. Sequence-specific determination of protein and peptide concentrations by absorbance at 205 nm. *Protein Sci. Publ. Protein Soc.* **22**, 851–858 (2013).

78. Kuete, V., Karaosmanoğlu, O. & Sivas, H. Chapter 10 - Anticancer Activities of African Medicinal Spices and Vegetables. in *Medicinal Spices and Vegetables from Africa* (ed. Kuete, V.) 271–297 (Academic Press, 2017). doi:10.1016/B978-0-12-809286-6.00010-8.

79. ab115347 Live and Dead Cell Assay_30 Jun 15b (website).pdf.

80. Bartelt, R. R., Cruz-Orcutt, N., Collins, M. & Houtman, J. C. D. Comparison of T cell receptor-induced proximal signaling and downstream functions in immortalized and primary T cells. *PloS One* **4**, e5430 (2009).

81. Liu, Y. *et al.* Genomic control of inflammation in experimental atopic dermatitis. *Sci. Rep.* **12**, 18891 (2022).

82. Hwang-Bo, J. *et al.* Parnassin, a Novel Therapeutic Peptide, Alleviates Skin Lesions in a DNCB-Induced Atopic Dermatitis Mouse Model. *Biomedicines* **11**, 1389 (2023).

83. Park, S. *et al.* Synthesis and biological evaluation of peptide-derived TSLP inhibitors. *Bioorg. Med. Chem. Lett.* **27**, 4710–4713 (2017).

84. Synthesis and biological evaluation of peptide-derived TSLP inhibitors - ScienceDirect. https://www.sciencedirect.com/science/article/pii/S0960894X17308880?via%3Dihub.

85. Bao, K. & Reinhardt, R. L. The differential expression of IL-4 and IL-13 and its impact on type-2 immunity. *Cytokine* **75**, 25–37 (2015).

86. Guo, L., Urban, J. F., Zhu, J. & Paul, W. E. Elevating Calcium in Th2 Cells Activates Multiple Pathways to Induce IL-4 Transcription and mRNA Stabilization1. *J. Immunol.* **181**, 3984–3993 (2008).

87. Pahl, A., Zhang, M., Kuss, H., Szelenyi, I. & Brune, K. Regulation of IL-13 synthesis in human lymphocytes: implications for asthma therapy. *Br. J. Pharmacol.* **135**, 1915–1926 (2002).

88. Ghasemi, M., Turnbull, T., Sebastian, S. & Kempson, I. The MTT Assay: Utility, Limitations, Pitfalls, and Interpretation in Bulk and Single-Cell Analysis. *Int. J. Mol. Sci.* **22**, 12827 (2021).

89. Hoogstraten, C. A., Smeitink, J. A. M., Russel, F. G. M. & Schirris, T. J. J. Dissecting Drug-Induced Cytotoxicity and Metabolic Dysfunction in Conditionally Immortalized Human Proximal Tubule Cells. *Front. Toxicol.* **4**, (2022).

90. Kusena, J. W. T., Shariatzadeh, M., Thomas, R. J. & Wilson, S. L. Understanding cell culture dynamics: a tool for defining protocol parameters for improved processes and efficient manufacturing using human embryonic stem cells. *Bioengineered* **12**, 979–996.

91. Ong, P. Y. Atopic dermatitis: Is innate or adaptive immunity in control? A clinical perspective. *Front. Immunol.* **13**, 943640 (2022).

92. Sideris, N. *et al.* New and Upcoming Topical Treatments for Atopic Dermatitis: A Review of the Literature. *J. Clin. Med.* **11**, 4974 (2022).

93. Lin, C. M., Cooles, F. A. & Isaacs, J. D. Basic Mechanisms of JAK Inhibition. *Mediterr. J. Rheumatol.* **31**, 100–104 (2020).

94. Chovatiya, R. & Paller, A. S. JAK Inhibitors in the Treatment of Atopic Dermatitis. *J. Allergy Clin. Immunol.* **148**, 927–940 (2021).

95. Dhillon, S. Delgocitinib: First Approval. *Drugs* **80**, 609–615 (2020).

96. Sadeghi, S. & Mohandesi, N. A. Efficacy and safety of topical JAK inhibitors in the treatment of atopic dermatitis in paediatrics and adults: A systematic review. *Exp. Dermatol.* **32**, 599–610 (2023).

97. Nakagawa, H. *et al.* Long-term safety and efficacy of delgocitinib ointment, a topical Janus kinase inhibitor, in adult patients with atopic dermatitis. *J. Dermatol.* **47**, 114–120 (2020).

98. Holthaus, L. *et al.* CD4+ T cell activation, function, and metabolism are inhibited by low concentrations of DMSO. *J. Immunol. Methods* **463**, 54–60 (2018).

99. Kragstrup, T. W. *et al.* Waiting for JAK inhibitor safety data. *RMD Open* **8**, e002236 (2022).

100. Gao, K., Oerlemans, R. & Groves, M. R. Theory and applications of differential scanning fluorimetry in early-stage drug discovery. *Biophys. Rev.* **12**, 85–104 (2020).

101. Alam, M. S. Proximity Ligation Assay (PLA). *Curr. Protoc. Immunol.* **123**, e58 (2018).

102. Siramshetty, V. B. *et al.* Retrospective assessment of rat liver microsomal stability at NCATS: data and QSAR models. *Sci. Rep.* **10**, 20713 (2020).

103. Indra, A. K. Epidermal TSLP: A trigger factor for pathogenesis of Atopic Dermatitis (AD). *Expert Rev. Proteomics* **10**, 309–311 (2013).

APPENDIX: SUPPLEMENTARY

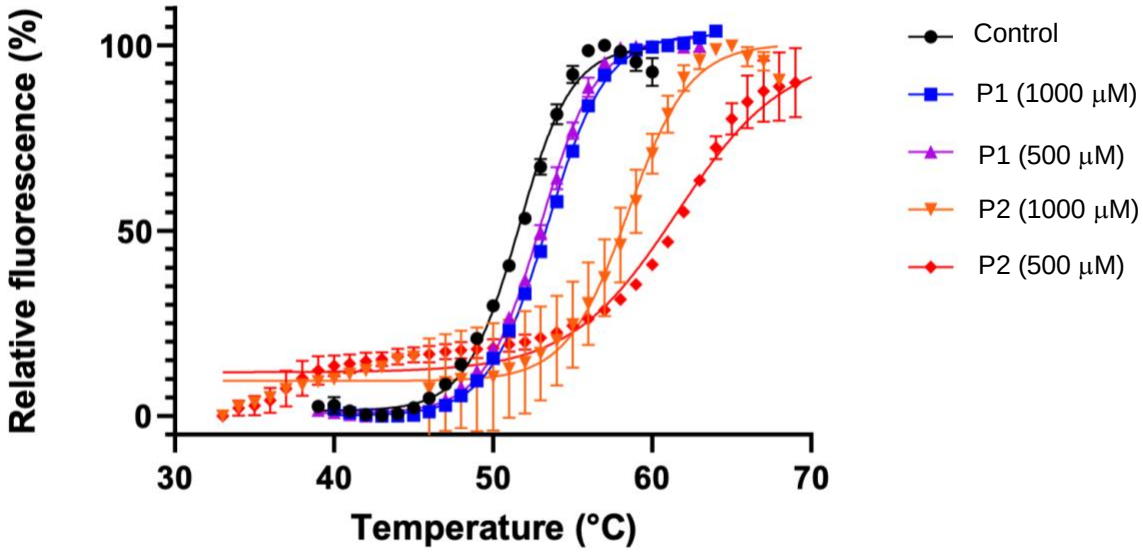

Sup 1. Binding of P1 and P2 to TSLPR using DSF. This data was collected by Dr. Temi Idowu.

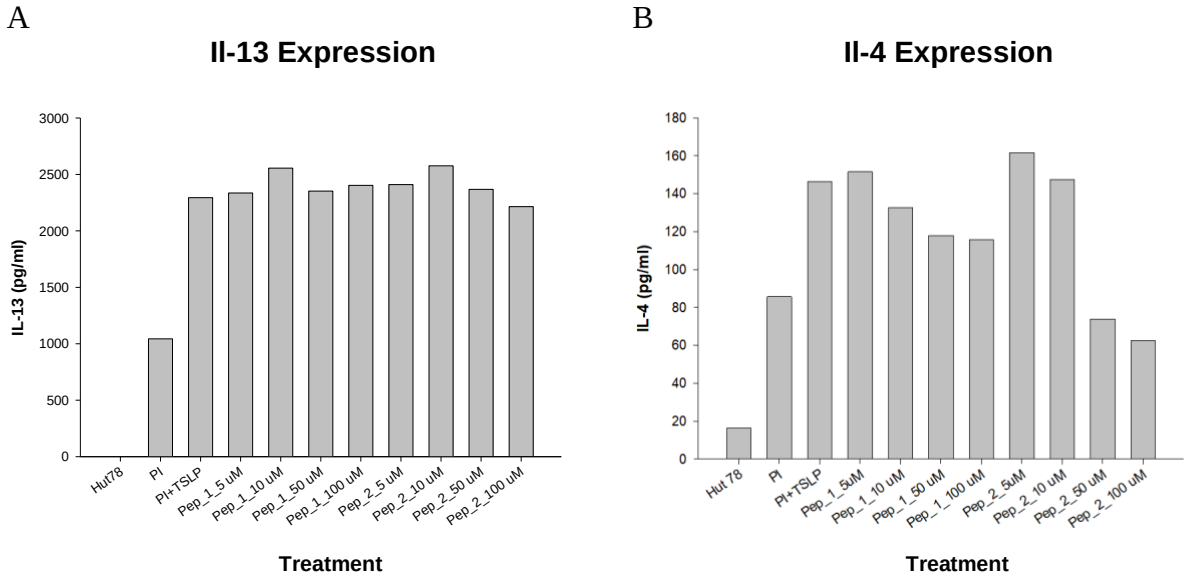

Sup 2. Inhibition of Th2 Cytokine Release by P1 and P2 in HUT78 Cells. The peptides were tested at 100 μM, 50 μM, 10 μM, and 5 μM and the effect on **(A)** Il-13 levels and **(B)** Il-4 levels were assessed. Pep_1 refers to P1 while Pep_2 refers to P2. This data was collected by Dr. Partho Adhikary.

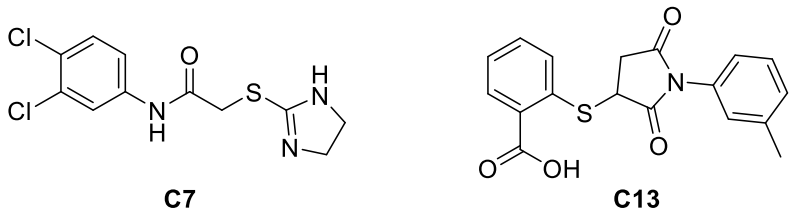

Sup 3. Chemical Structures of C7 and C13.

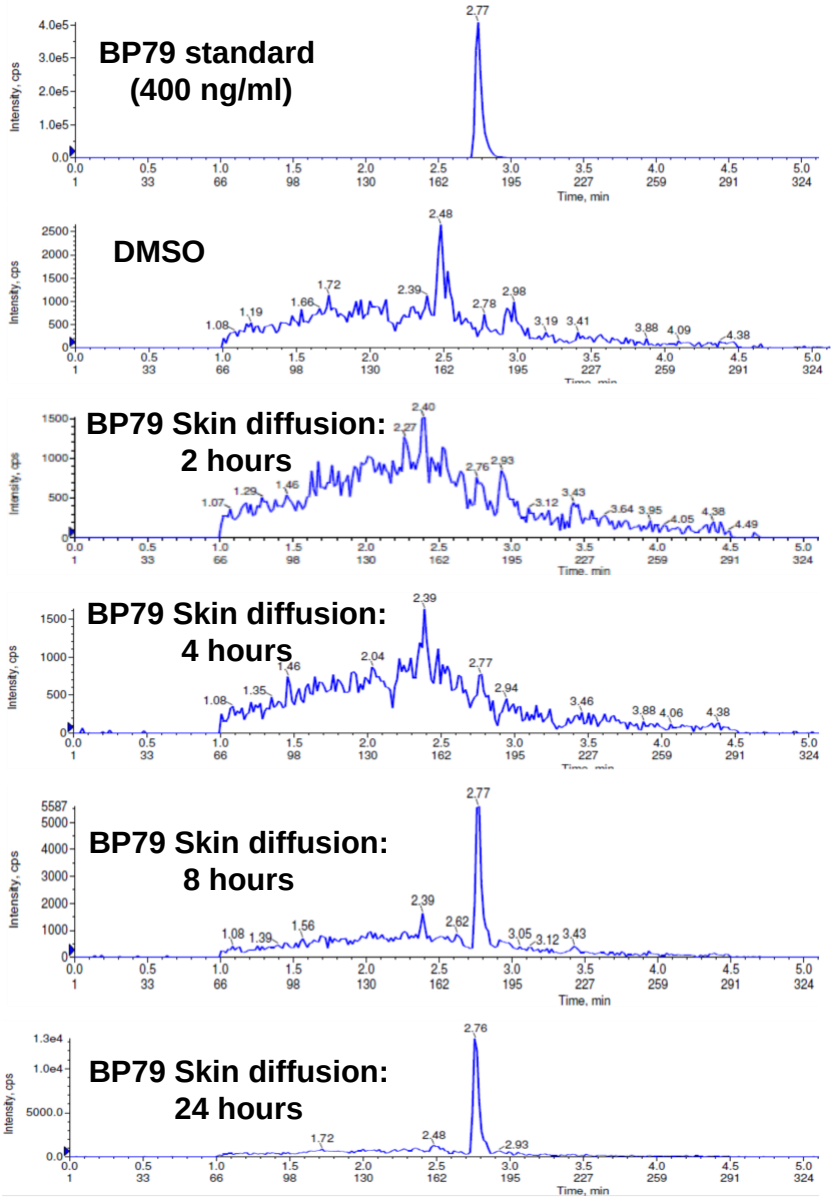

Sup 4. Skin penetration of BP79

Compound	R		Compound	R
BP252	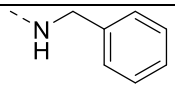		BP243	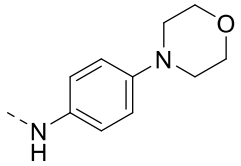
BP253	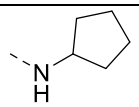		BP262	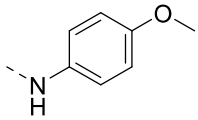
BP254	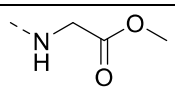		BP263	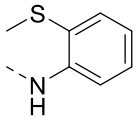
BP255	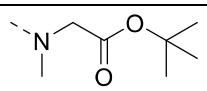		BP264	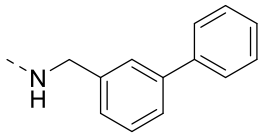
BP256	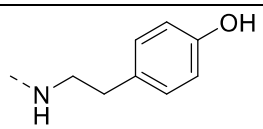		BP265	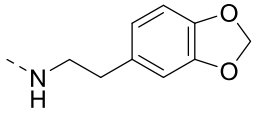
BP257	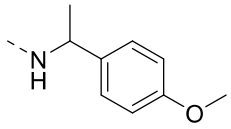		BP266	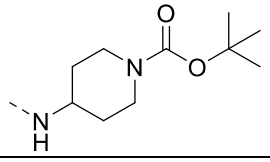
BP258	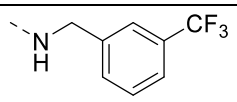		BP267	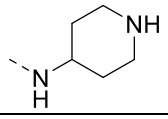
BP259	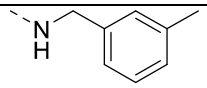		BP268	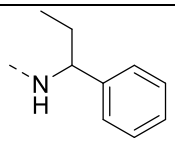
BP260	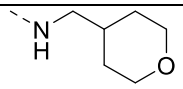		BP270	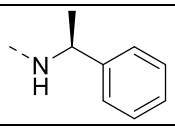
BP261	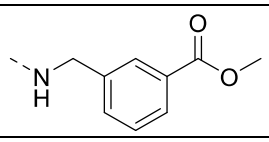		BP271	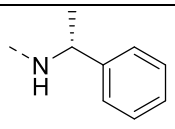
BP269	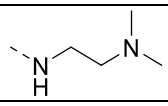		BP272	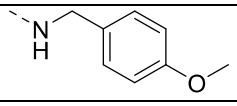

Compound	R
BP273	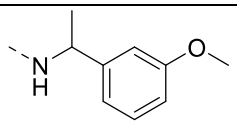
BP274	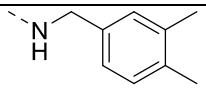
BP275	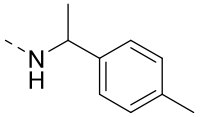
BP276	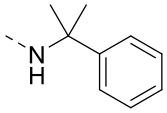
BP277	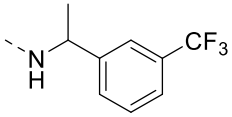
BP287	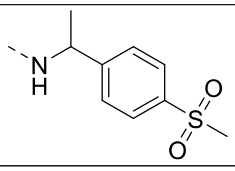

Sup 5. Chemical Structures of BP79 Analogues.